ANNI SIITONEN

SPECTROSCOPIC STUDIES OF SEMICONDUCTING SINGLE-WALLED CARBON NANOTUBES

Academic Dissertation for
the Degree of Doctor of Philosophy

UNIVERSITY OF JYVÄSKYLÄ

2010

SPECTROSCOPIC STUDIES OF SEMICONDUCTING SINGLE-WALLED CARBON NANOTUBES

BY

ANNI SIITONEN

Academic Dissertation
for the degree of
Doctor of Philosophy

To be presented, by permission of the Faculty of mathematics and Science of the University of Jyväskylä, for public examination in Auditorium FYS1, on November 19th 2010, at 12 noon.

UNIVERSITY OF JYVÄSKYLÄ

ABSTRACT

The unique nature of optical properties of single-walled carbon nanotubes (SWCNT), together with their promising potential applications, have created enormous interest towards the photophysics of SWCNT. Many aspects of carbon nanotubes originate from the electronic structure of carbon honeycomb lattice and one-dimensionality. SWCNTs exist in various chiral structures and diameters, which the optical and electrical properties are dependent on. It has been discovered that SWCNT excited states are excitonic with strong Coulomb interaction between the electron and the hole. However, many features of excitons are not yet well defined, such as absorption cross-sections, fluorescence quantum yields, exciton lifetimes, and the nature of exciton mobility. The cylindrical shape with all atoms on the surface makes SWCNTs highly sensitive to environment which is a significant factor affecting the optical properties.

   First part of this thesis concentrates on the temperature dependence of excitonic absorption transitions. The importance of this study lies in the complexity of environmentally induced mechanisms to alter the energy gap and shift the electronic absorption transitions as a function of temperature. The results revealed abrupt shift in the energy gap interpreted to originate from interactions with water. The second part discusses the processes occurring after absorption: exciton mobility and dynamics. By analyzing reactions between single-molecule diazonium salt and individual nanotubes, the distance travelled by exciton during its lifetime, in different surfactants and for different chiral structures was determined. The results indicate that localized excitons have diffusional motion along the nanotube axis. The large diffusion ranges obtained (160 - 340 nm) explain the sensitivity of SWCNT emission to changes in local environment. The dynamics of excitons were studied with excitation dependence measurements. Results revealed the existence of long lived states that act as quenchers of emission even at relatively low excitation intensities.

Keywords: carbon nanotubes, Fourier transform infrared (FTIR) spectroscopy, fluorescence spectroscopy, fluorescence microscopy, exciton diffusion, exciton dynamics

4

Author's address   Anni Siitonen
Department of Chemistry
University of Jyväskylä
Finland

Supervisors   Adjunct Professor Mika Pettersson
Department of Chemistry
University of Jyväskylä
Finland

Professor Henrik Kunttu
Department of Chemistry
University of Jyväskylä
Finland

Reviewers   Professor Achim Hartschuh
Department of Chemistry
Ludwig-Maximilians-University of Munich
Germany

Professor Markku Räsänen
Department of Chemistry
University of Helsinki
Finland

Opponent   Professor Tobias Hertel
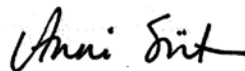Institute for Physical Chemistry
University of Würzburg
Germany

PREFACE

I have been privileged to do my research surrounded by many brilliant and enthusiastic people. Firstly, I wish to thank my supervisor Adj. Professor Mika Pettersson who has given me talented guidance and tremendous support. I highly appreciate the never-ending positive attitude and energy you have. I feel lucky having you as my advisor. My gratitude extends to Professor Henrik Kunttu for encouraging me throughout the years and providing valuable advice in the final stage of the thesis. I also want to acknowledge all the dear colleagues in the Nanoscience Center who are responsible for making the work so pleasant.

I want to express my warmest thanks to Professor Bruce Weisman for giving me the opportunity to work at Rice. Those two years were extremely educational and exciting for me and it has been an honor working with you. Dr. Sergei Bachilo I want to thank for all the passionate and friendly discussions we had about nanotubes, excitons and everything else. Enormous appreciation goes to Dr. Dima Tsyboulski. Thank you for all your hard work and endless help and support that carried me through the challenging projects.

I wish to acknowledge all my precious friends that I have been lucky to have for many years. Thank you for being there for me and sharing the joys of life with me. Finally, I express my deepest thanks to my family for their warmest support - my mother Raija, father Heikki, sister Jenni, brother-in-law Janne and my loveliest niece Anniina. And last but not least, thank you so much for so many things, Dan.

Jyväskylä, October 2010

Anni Siitonen

LIST OF ORIGINAL PUBLICATIONS

This thesis is a review based on the original publications and a manuscript listed below and they are herein referred to by their Roman numerals.

I **Temperature dependence of electronic transitions of single-wall carbon nanotubes: Observation of an abrupt blueshift in absorption.**
A. Siitonen, H. Kunttu and M. Pettersson, *J. Phys. Chem. C.* **2007**, *111,* 1888-1894
Correction: *J. Phys. Chem.* C **2007**, *111*, 11500

II **Surfactant-dependent exciton mobility in single-walled carbon nanotubes studied by single-molecule reactions**
A. J. Siitonen, D. A. Tsyboulski, S. M. Bachilo, R.B. Weisman, *Nano Lett.* **2010**, *10,* 1595-1599

III **Dependence of exciton mobility on structure in single-walled carbon nanotubes**
A. J. Siitonen, D. A. Tsyboulski, S. M. Bachilo, R.B. Weisman, *J. Phys. Chem. Lett.* **2010**, *1,* 2189-2192.

IV **Excitation intensity dependent measurements of single-walled carbon nanotubes**
A. J. Siitonen, S. M. Bachilo, D. A. Tsyboulski, R.B. Weisman, manuscript

Author's contribution

In Paper I, the author has had a major role in all measurements and analysis of experimental data and has written chapter "Experimental methods".

In Papers II, III and IV, the author has had a major role in all the measurements, analysis of experimental data and writing of the manuscripts.

ABBREVIATIONS

CVD	chemical vapor deposition
DMF	dimethylformamide
EEA	exciton-exciton annihilation
FTIR	Fourier transform infrared
HiPCO	high pressure CO conversion
NIR	near infrared
ODCB	ortho-dichlorobenzene
PL	photoluminescence
PLE	photoluminescence excitation
RBM	radial breathing mode
SC	sodium cholate
SDBS	sodium dodecylbenzenesulfonate
SDC	sodium deoxycholate
STC	sodium taurocholate
SWCNT	single-walled carbon nanotube
UV	ultraviolet
VIS	visible

SISÄLLYS

1 INTRODUCTION

Carbon is an intriguing element, a "true genius" as Nobel laureate Richard Smalley described. It is one of the few elements known since antiquity, yet it still is able to challenge and amaze scientists today with its remarkable properties. Carbon can exist in different forms, allotropes, depending on the physical conditions carbon is put under. Diamond and graphite have been well-known for thousands of years and after beginning of nanoscience the carbon family has grown with new members: fullerene, carbon nanotube and graphene. These carbon nanostructures are under enthusiastic studies because of their promising applications in all fields of science- biology, chemistry and physics.

This thesis concentrates on carbon nanotubes, a unique structured material discovered about 20 years ago. This material has created intense interest among scientists after its remarkable properties were discovered. Carbon nanotube is one of the hardest materials in the world, with excellent strength to weight ratio. It has high thermal and electric conductance with limited scattering. In addition it has unique optical properties arising from one dimensionality. Due to such outstanding qualities, the expectations towards potential applications are immense. At the moment carbon nanotube is commercially used for example in ice-hockey sticks and skis, making them strong but light in weight. However, these applications are just a modest start. Some of the most exciting future scenarios include strong lightweight components for spacecrafts, robots moving with artificial muscles or nanodevices for selective drug delivery.

Before such designs can be executed, there are various challenges that need to be overcome by scientists. This thesis presents the efforts made for understanding the complex nature of optical properties of carbon nanotubes. The work has been carried out at University of Jyväskylä and Rice University during 2006 - 2010.

2 SINGLE-WALLED CARBON NANOTUBES AND THEIR SPECTROSCOPY

The first study presented in this thesis concentrates on excitonic absorption. The second part discusses the processes occurring after absorption: exciton mobility and dynamics. A significant and common theme in both studies is the environmental effect. This chapter presents some key factors in nanotube spectroscopic studies providing motivation for the work done in this thesis.

2.1 General features of SWCNTs

Single-walled carbon nanotube (SWCNT) has a geometrical shape of a cylinder wrapped from a sheet of graphene (see Figure 2.1). The graphene sheet can be rolled as a tube in various ways, resulting in distribution of different structures and tube diameters. The diameters of the tubes are around 1 nm whereas the length can be micrometers or even millimeters, making carbon nanotube a one dimensional (1D) structure defining a variety of its unique properties. Carbon nanotubes are generally referred as single molecules or quasi-1D crystals with transitional periodicity along the tube axis.
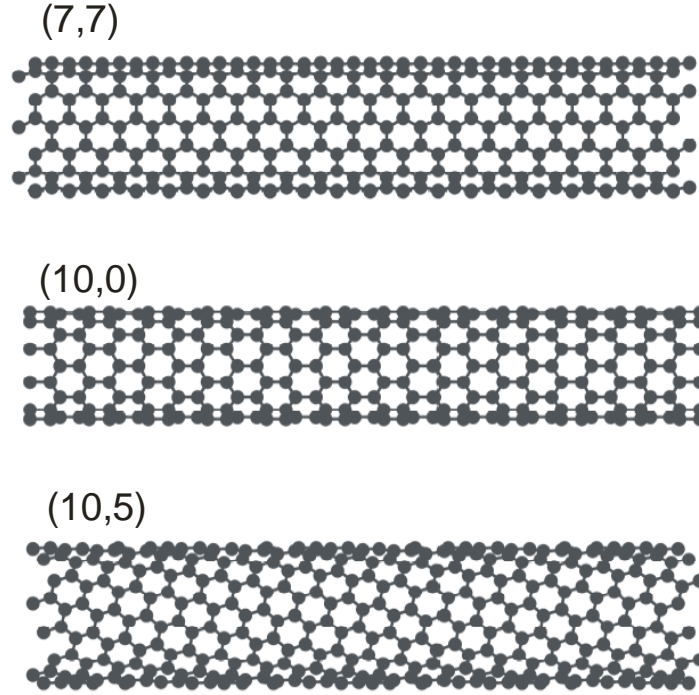
(7,7)

(10,0)

(10,5)

Figure 2.1 Theoretical models of SWCNTs with different structures: (7,7) "armchair", (10,0) "zigzag" and (10,5) "chiral".

In bulk SWCNT samples a continuous distribution of diameters and structures is represented. The structure is defined unambiguously with the roll-up vector C_h defined as $C_h = n\bar{a}_1 + m\bar{a}_2 = (n,m)$ where indexes n and m are multipliers of unit vectors of graphene $\bar{a}_1$ and $\bar{a}_2$ (see Figure 2.2). The direction of roll-up vector is defined by the angle between chiral vector C_h and unit vector $\bar{a}_1$ and it can vary between $0°$ and $30°$. All tubes except armchair (n,n) and zig-zag $(n,0)$ are chiral, in other words they are congruent with their mirror reflection. Many electronic and optical properties of SWCNTs are dependent on the structure. The semiconducting carbon nanotubes can be assigned into families according to the value of n-m and into subsets according to the value, 1 or 2, of remainder (mod) of n-m divided by 3.[1-3] From hereinafter the subsets are referred to as "Mod 1" and "Mod 2", respectively. Nanotubes belonging to the subset "mod 3 = 0" are metallic and excluded from this study. The roll-up vector also defines the tube diameter, by equation

$$d = \frac{|C_h|}{\pi} = \frac{a\sqrt{n^2 + nm + m^2}}{\pi}$$
Equation 2.1

where $a = 1.42\sqrt{3}$ Å is the lattice constant of graphene.

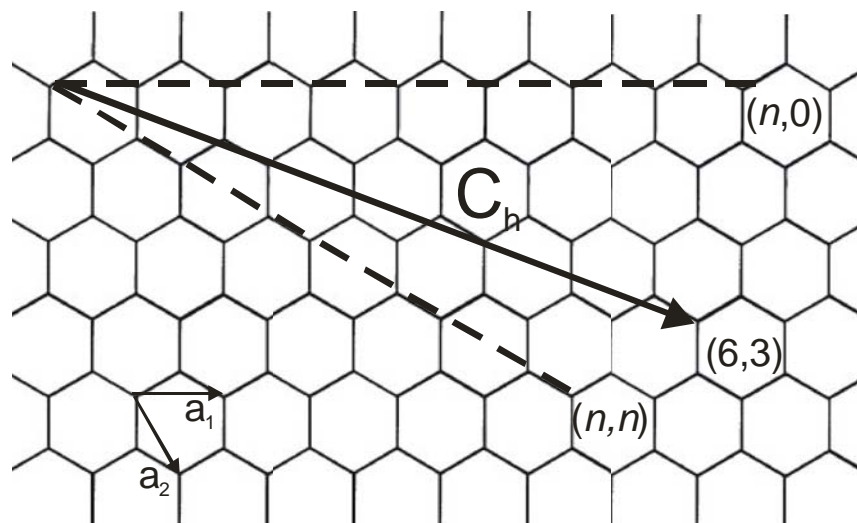**Figure 2.2** Schematic of a 2-dimensional graphene sheet illustrating unit vectors $\overline{\mathbf{a}}_1$ and $\overline{\mathbf{a}}_2$, and the roll-up vector C_h. The achiral cases of $(n,0)$ "zigzag" and (n,n) "armchair" are indicated with dashed lines.

Bulk SWCNTs can be produced with various methods e.g. laser-ablation,[4] electric arc technique[5] and chemical vapor deposition[6] (CVD). In the first two methods the reactants used are solid carbon compounds which then are evaporated at high temperatures, and powdered samples with nanotubes tangled into bundles can be produced. In CVD, which is the most common industrial method, nanotubes are grown from gaseous carbon compounds on top of metallic particle catalysts. Tubes made with this technique are better separated, and can even be suspended as individuals across trenches. Various CVD methods differ by the gaseous reactant used, like methane[7] and alcohols[8]. HiPCO, standing for high-pressure catalytic decomposition of carbon monoxide[9] is the most efficient production method known today, producing a kilogram per day of SWCNTs with low proportion of amorphous carbon. Further development of HiPCO method has been provided by the CoMoCat process.[10] The method involves using of cobalt and molybdenum bimetallic catalysts to produce SWCNTs with high selectivity of chiral structure. All the methods described produce samples with a range of nanotube diameters and structures. The bulk SWCNT samples include impurities such as amorphous carbon, metallic catalysts, carbon nanoparticles, multi-walled and double-walled tubes, and their percentage varies according to synthesis procedure. There are several methods of purification varying according to impurities present. Many methods include ultrasonication treatment which is known to cut SWCNTs to shorter species. The range of nanotube diameters in bulk sample vary according to synthesis method and physical conditions like temperature and pressure. Also the percentage of metallic/semiconducting tubes may vary. The significance of synthesis, impurities and purification are to be considered when doing research with bulk SWCNTs, whereas many of these

problems can be neglected when working with individual tubes. The development of synthesis methods and controllability of the process towards more uniform samples is essential for advancements in nanotube applications.

2.2   Optical properties of SWCNTs

Optical properties of SWCNTs are of significant interest from the point of view of many potential applications. SWCNTs also serve as models for studying physical effects in quasi-one-dimensional quantum systems. The predicted electronic band structure consists of sharp van Hove singularities arising from quasi-one dimensionality of semiconducting species (see Figure 2.3). Initially the optical transitions of SWCNTs were considered as band-to-band electronic transitions between these sub-bands. The dominant optical electronic transitions for excitation light polarized along the nanotube axis connect bands with the same index, labeled E_{ii}, (i =1, 2, 3,..) whereas the transverse transitions are strongly suppressed.[11] This model described successfully the general trends observed. By combining theoretical and experimental results the dependence of the two lowest energy transitions E_{11} and E_{22} on diameter[12, 13] and on structure[14] was confirmed, indicating that each (n,m) structure has unique E_{22} absorption and E_{11} emission combination.
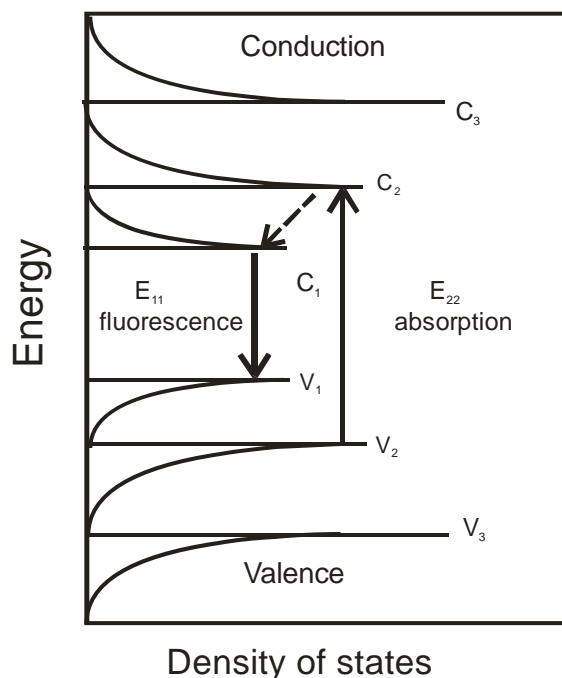

Figure 2.3 Density of electronic states for a single nanotube structure consisting of van Hove singularities. Band-to-band transitions are indicated with arrows. Solid arrows depict the optical excitation and emission transitions of interest; dashed arrow denotes non-radiative relaxation from C_2 to C_1.

Bachilo et al. used the band-to-band model to assign optical spectra of SWCNTs to specific (*n,m*) structures.[1] They excited ensemble sample of HiPCO SWCNTs dispersed in water soluble surfactant with electromagnetic radiation at wavelengths 300-930 nm coincident with E_{22} resonant absorption of semiconducting tubes and measured photoluminescence (PL) of E_{11} in near-infrared (NIR) (810 - 1550 nm). The Photoluminescence Excitation (PLE) Map revealed intriguing pattern of spots each representing a single (*n,m*) species (see Figure 2.4). The PLE map was analyzed against resonant Raman radial breathing modes (RBM). These modes are strongly and selectively enhanced when the photon energy matches the optical transition of SWCNT and are known to have monotonic relation to tube diameter. The study resulted in assignment of absorption and PL spectra to specific (*n,m*) species and a formula to predict (*n,m*) structure from resonant absorption and PL energies.[1, 15] Since that study, PL spectroscopy has become the strongest tool for reliable characterization of semiconducting nanotube structures.
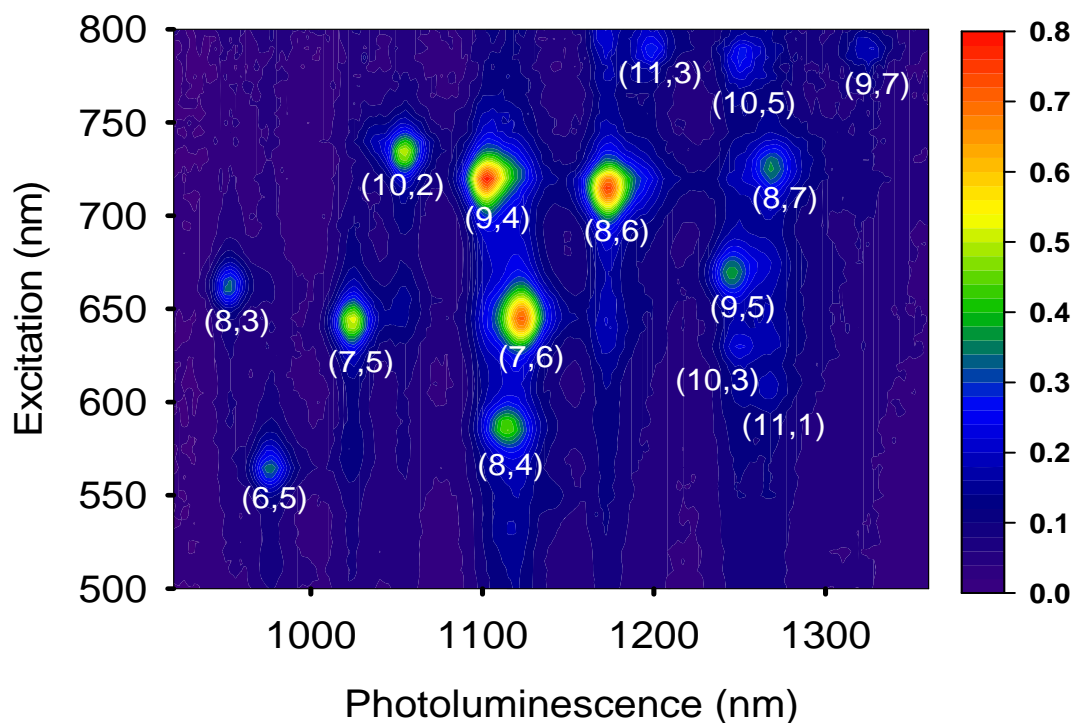

Figure 2.4 Two dimensional contour plot of PL intensity versus excitation and emission wavelengths. Each bright spot represents emission from certain (*n,m*) structure, as identified in the plot according to Bachilo et al.[1]

However, the correct assignment of chiral indexes revealed irreconcilable differences between the calculated band-to-band and experimental energies, known as the "ratio problem". The band-to-band model predicted that the ratio of energies E_{22}/E_{11} for smaller diameter tubes is < 2 due to diameter dependent curvature effects, but should approach 2 in the limit of large diameters.[2] On the other hand, the experimentally obtained ratio approached a value less than 2. The simple model excluding Coulombic interactions between the electron and the hole was not enough and reconciliation to the ratio problem came through an excitonic model described earlier by Ando.[16] Coulomb interaction gives rise to several bound excitonic states and changes the energy gap. The ratio problem was explained by one-dimensionality of carbon nanotubes which makes the electron-hole interactions particularly strong.[17] The direct evidence of excitonic nature of optical transitions in SWCNTs was obtained experimentally ruling out the band-to-band transitions.[18] The Coulomb interaction in three dimensional conducting species is typically decreased by dielectric screening (i.e. mobility of charges). In nanotubes the motion of particles is restricted to one dimension and the electric field generated by the electron-hole pair is largely outside of the tube decreasing the screening effect. Consequently, due to one dimensionality, the probability for short electron-hole separations is relatively more important than long separations (vice versa for higher dimensional species), enhancing the role of the Coulomb interaction. Because of these factors, the Coulombic interaction in SWCNT is relatively strong with binding energies of 0.3 - 0.4 electron volts,[18-20] indicating that excitons in SWCNTs have Frenkel type character. However, excitons in SWCNT are not localized around an atom, but electron-hole distance is much greater than SWCNT lattice constant, indicating Mott-Wannier exciton type typical for semiconductors. Size of exciton in SWCNTs has been estimated to be ~2 nm, a value larger than the nanotube diameter.[21, 22] Furthermore, excitons have noticeable mobility along the nanotube axis. The length of exciton excursion during its lifetime has been measured to be 6 nm and 100 nm. [21, 23] Hereinafter the excitonic states E_{ii} are labeled according to the transitions.
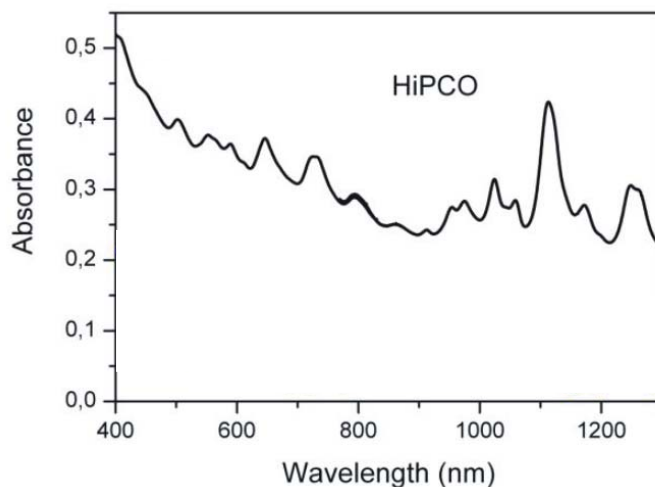
Figure 2.5 Typical absorption spectrum of HiPCO SWCNTS dispersed in dimethylformamide (DMF). The near-infrared region ~750 - 1400 nm consists of E_{11} absorption peaks arising from specific semiconducting (*n,m*) structures. The visible region consist of absorption peaks arising from both semiconducting and metallic SWCNTs.

Despite recent developments, the photon absorption as well as physical processes occurring after photoexcitation are not yet fully understood. The E_{22} absorption transitions of semiconducting SWCNTs take place in the visible spectral region. Typical absorption spectrum of ultrasonicated and ultracentrifuged SWCNT ensemble sample in dimethylformamide (DMF) is represented in Figure 2.5. At visible spectral region ~400 - 700 nm, some structure is observed in addition to continuum rising towards higher energy. Absorption at this region is a combination of higher excitation states of semiconducting SWCNTs, absorption of metallic tubes, metallic particles and amorphous carbon. In the near-infrared (NIR) region ~750 - 1400 nm (~13000 - 7000 cm^{-1}) the absorption transitions of semiconducting SWCNTs arising from different nanotube structures are observed as better resolved absorption peaks.

The probability of an absorption process can be described by absorption cross-section. A value of 0.6 - 1.8*10^{-17} cm^2 per carbon atom has been deduced for only few structures.[24, 25] When looking at the relative PL intensities from PLE maps (see Figure 2.4) it is noticed that the intensities for group Mod 1 are lower than for Mod 2. Since the concentration of each structure is not known in the bulk samples, this leads to suggestion that the decrease in brightness is due to lower abundance of those tube structures. However, since the synthesis processes are not highly selective, it is unlikely that there is a strong tendency towards a certain subset of structures. Oyama et al. studied the phenomenon by comparing theoretical calculations with experiments.[26] They predicted that absorbance and PL intensities are structure-dependent and show a trend within families. Absorbance for Mod 2 structures was predicted to be higher than for Mod 1. This has not yet been fully proven by experimental studies.
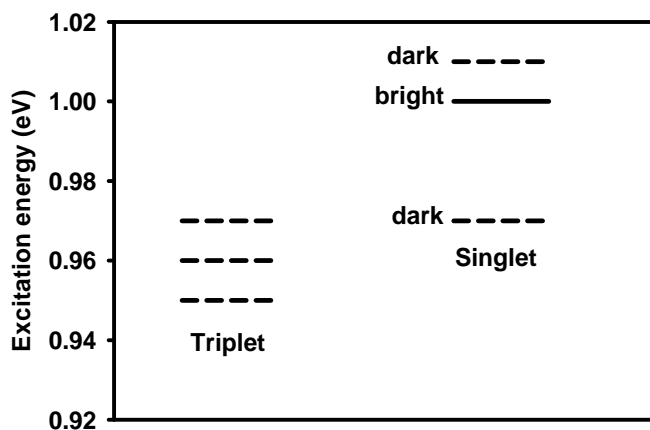
Figure 2.6 The excitonic energy sublevels for (10,0) SWCNT according to Spataru et al.[27]

The PL intensity of SWCNTs involves a combination of initial photon absorption, relaxation from E_{22} to E_{11} and photon emission. These processes are likely to have components dependent on intrinsic as well as extrinsic effects. The relaxation from higher excited states to E_{11} occurs non-radiatively via exciton-phonon interaction with much faster rate than emission E_{11}.[26] The intersubband relaxation rate from higher exciton states to E_{11} has not yet been determined with good accuracy for individual nanotubes. After relaxation, the excitons are formed and distributed within excitonic energy sublevels (see Figure 2.6). The E_{11} excitonic singlet-state is a bright state with odd parity and angular momentum k = 0.[27-29] Above this state lies a doubly degenerate even-parity singlet state with k = ±1, which is dipole-forbidden for optical transitions, and thus a dark state. Another important dark state with even parity and k = 0 lies below the bright state. Triplet states lie lower in energy. The distribution of excitons on these states described here is still an intriguing question. The theory predicts that in an ideal nanotube the excitons do not scatter between states of different parities[28] but the decrease in PL intensity below 50 K could suggest symmetry-breaking by environment allowing equilibrium between dark and bright exciton states.[30, 31] The existence of dark excitonic states has been observed under high magnetic fields as bright states and dark states with zero angular momentum are mixed.[32, 33] This phenomenon is weak at room temperature suggesting thermal equilibrium between dark and bright excitonic states, but gets stronger below 50 K. The existence of dark states explains the low efficiency of light emission of semiconducting SWCNTs. The efficiency is described with PL quantum yield defined as ratio of the number of photons emitted to the number of photons absorbed. The PL quantum yields are approximated to be less than 0.2.[34-36] Furthermore, a study of PL action cross-section (absorption cross-section* PL quantum yield) indicate substantial structure dependence.[35] However, conclusive quantum yields have not been defined yet.

Exciton dynamics is affected by non-radiative processes with phonons, surface defects and impurities as well as exciton-exciton interactions. The relatively low quantum yield suggests that exciton dynamics is dominated by non-radiative processes, coinciding with long radiative lifetimes obtained, 10 and 110 ns.[37, 38] However, whether the long lifetimes arise from intrinsic, extrinsic or both effects, remains to be revealed. The difficulties in answering these questions are connected with the challenges in sample preparation, environmental effects and inhomogeneities of bulk/ensemble samples. The short and long components of exciton lifetimes measured from ensemble samples are 0.3 - 45 ps and 5 - 250 ps, respectively.[39-42] The variations are likely due to influence of suspension medium[43] as well as differences in experimental methods. The lifetimes measured from individual (*6,5*) tubes in aqueous gel environment have components 10-65 and 200-800 ps.[44, 45] A three level model including a ground state and bright and dark excitonic states was used to explain these PL decays. In recent study, (6,5) and (6,4) tubes in two different environments were measured and both mono- and biexponential PL decays were observed.[46] The proportionality of monoexponential decays increased in the more heterogeneous environment for (6,5). The processes of exciton-exciton interactions become crucial at excitation levels sufficient to create two or more excitons in a tube within exciton lifetime. The interactions are significant due to substantial movement of excitons. Typically excitons collide via exciton-exciton annihilation (EEA) opening at the same time a non-radiative decay channel that relatively decreases the density of excitons and is observed in excitation intensity dependence measurement as nonlinearity. The early studies on EEA suggested that the interaction process is of Auger type[42], i.e. electron-hole pair annihilates and releases its energy to third party charge carrier. The study suggests the existence of free electron or holes arising from intrinsic or extrinsic factors, inducing annihilation of exciton with Auger process. The Auger process has been useful in describing nonlinearity in experimental work where excitation is done with pulsed lasers.[20, 25] However, measurements with continuous excitation proved that nonlinearity is observed at such low intensities that exciton-exciton interactions are negligible.[24] The cause of this non-linearity is not yet determined.

2.3 Extrinsic and intrinsic aspects in SWCNT spectroscopy

Since all carbon atoms in SWCNT are on the surface all physical and chemical properties, including absorption and emission, are dependent greatly on the immediate environment of SWCNT. There are various extrinsic effects, such as physical conditions, neutral or ionic surfactant coating, substrate, solid matrix or air/gas suspension. Important phenomena are weak van der Waals interactions of SWCNTs with each other and their tendency to bundle. Nanotube bundles consist of tubes with different chiralities and diameters.[47, 48] Bundling has a tendency to change nanotube properties such as electronic

transitions and makes absorption bands wide and non-characteristic. PL is especially sensitive to bundling effects explaining the late observation of SWCNT emission, 10 years after the discovery of nanotubes.[49] The crucial step to observe PL was ultrasonication and centrifugation treatment of SWCNTs in water and surfactant. Sonication breaks the nanotube bundles and surfactant forms a micelle surrounding individual tubes. Only after discovery of this procedure the absorption and emission spectra with well separated peaks were observed. However the intensity of PL is sensitive to the type of surfactant,[43] possibly according to the surfactants tendency to wrap around the tube and to hinder interaction with water. Electronic transitions are also pH dependent.[50] Electrostatic doping removes/adds electrons from/to resonant states and light absorption is suppressed at pH <5. Absorption is mainly sensitive to state filling, but PL is very sensitive to dopants as reactive centers. Excitons move towards dopant centers causing dramatic suppression of PL. This has been demonstrated by stepwise quenching of PL after addition of acid, measured from an individual SWCNT.[23] When attached to a solid material, the PL is quenched, since interaction with environment offers additional non-radiative relaxation path.

In addition to extrinsic, also intrinsic effects can hamper spectroscopic studies of SWCNTs. Firstly, images of SWCNTs recorded with scanning tunneling microscope reveal that not all nanotubes are pristine but instead of having hexagonal lattice structure, the tube can consist of heptagon-pentagon junctions that naturally influence the electronic structure of tubes.[51] Secondly, there are physical defects caused by treatment of samples, mainly ultrasonication, used for dispersion of tubes. Ultrasonication is a strong method and, in addition to debundling, it can damage tubes and cut them shorter. Defects as well as nanotube ends can act as reactive sites and hamper nanotube emission measurements by quenching the PL intensity.

The dependence of absorption and emission properties on physical parameters such as temperature, electric field and magnetic field has also been widely studied.[31, 52, 53] The sensitivity of electronic transitions to temperature effects are highly significant and should be taken into account when theoretical results, often calculated at 0 K, are used to explain experimental observations. In addition, temperature dependence of band transitions can provide further information about electronic structure, for example coupling between electrons and phonons. Theoretical study predicts small diameter- and structure-dependent negative shifts in band gap energies at 300 K for individual nanotubes.[54] Similar observations were made with tunable Raman spectroscopy[55] and PL spectroscopy[31, 56] with the sign of the shift depending on the tube structure. Fantini et al. reported that E_{22} transition energies for semiconducting SWCNTs are redshifted and blueshifted for Mod 2 and Mod 1, respectively, while increasing the temperature.[57] The observation indicates interesting difference in behavior between the two subset. The strain induced to nanotube due to its surroundings, such as surfactant wrapping or bundling with other tubes[31, 55, 56] as well as adsorption and desorption of gases[58, 59] can

cause positive or negative abrupt energy shift. These studies have again proven how diverse the environmentally induced mechanisms affecting the complex electronic structure of SWCNT indeed are.

The environmental effects discussed in this chapter together with impurities (metal particles, multi- and double-walled tubes, amorphous carbon) and large distribution of various structures (metallic and semiconducting) and lengths have had enormous impact on all SWCNT studies. Many results measured from bulk or ensemble samples have been hampered with several uncertainties that can be avoided when combining spectroscopic and microscopic techniques.[35, 44, 60] For example with fluorescence microscope, one individual semiconducting SWCNT can be imaged and characterized by comparing the wavelength of emission spectrum to PLE map (see Figure 2.4). From the shape, width and position of the peak it is possible to evaluate with good certainty whether the tube is individual or bundled. Bundled tubes are observed as multiple peaks or as a shift in peak position.[61] The full-width of half-maximum values are approximately 30 cm^{-1} larger for bulk samples than for individual SWCNT[34] though varying according to structure and surfactant. Defects can be evaluated visually and tubes that show no observable dark areas can be assessed as nearly pristine. The instability of PL intensity can reveal that there are possible impurities in the vicinity of the tube, though not visible in fluorescence image.

2.4   SWCNTs in applications

SWCNT is extremely promising material for industrial applications with its unique mechanical and thermal properties. The graphitic sp^2 hybridized carbon-carbon bond makes nanotubes one of the hardest material, 33 % stronger than the hardest material in nature, diamond.[62] Unlike planar graphene, nanotubes with cylindrical shape have structural stability also under compression. Spinning nanotubes into yarns and fibers could result in most stiff material. Thermal conductivity along axis of nanotube, derived from strength and toughness of sp^2 bond and 1D character that limits the scattering processes, appears to be superior to other materials. Nanotube structures are stable up to 4000 K. In addition, carbon is light material compared to many metals. These remarkable thermal and mechanical properties provide carbon nanotubes tremendous possibilities in applications. For example, nanotubes can replace carbon-fiber composites and graphite to increase the strength of such materials. Applications vary from aerospace devices to everyday sporting goods. Carbon nanotubes have potential to replace metals in heat transport with decreasing heat losses. They can potentially be applied to conducting thin films, solar cells, artificial muscles, nanoscale electrodes and components of nanostructured field effect transistors and single electron transistors. Conductance of nanotubes is highly sensitive to environmental changes providing great potential usage as

sensors. Other prospective applications of SWCNTs are NIR light emitting diodes in nanoscale devices.

Some especially promising applications arise from sensitivity of semiconducting SWCNT PL, such as sensing and imaging in biological systems as well as nanomedicine and therapeutics. For biomedical applications, SWCNTs have a number of advantages: 1) they are optically stable and do not photobleach 2) they are sensitive to changes in dielectric environment because all the atoms in SWCNT are on the surface 3) they have high absorbance at visible spectral region where water is most transparent and 4) SWCNTs fluoresce in near- infrared, a region of light spectrum where blood and tissue are most transparent. Pioneering work has been done demonstrating promising results of sensitive and selective fluorescent nanosensor for detection of DNA,[63] glucose,[64] hydrogen peroxide[65] and nitric oxide[66] even at single molecule level. Some experiments show promising results for *in vivo* imaging in mouse.[63-66]

Today there are still several challenges that need to be overcome before carbon nanotubes can be effectively used in industrial applications. One is production of high-quality nanotubes with efficient and low-costing techniques. Also there are challenges involving the heterogeneity of the material and difficulties in achieving uniform dispersion and well-aligned nanotubes. SWCNT ensemble samples consist of a wide variety of different structures, whereas many applications would require samples consisting of only one type of structure. Significant steps towards separation of such samples have been made through density-gradient ultracentrifugation.[67-70] The technique is based on sorting of nanotubes according to diameter, energy gap and electronic structure using structure-discriminating surfactants to create species with subtle differences in their densities. Another promising approach has been the creation of DNA/SWCNT hybrids that are selective according to DNA sequences and structure.[71, 72] Over 20 DNA sequences have been identified to selectively disperse 12 semiconducting SWCNTs. Both methods are under abundant study and show promising development towards manipulation of SWCNTs in various environments. Furthermore, many fundamental properties of nanotubes are not yet understood and intensive research still needs to be focused on basic research of this material. Increasing importance is also put on safety aspects of carbon nanotubes.

3 EXPERIMENTAL METHODS

3.1 Experiments with near-infrared absorption spectroscopy

The study of temperature dependence of absorption transitions was performed with material prepared by CVD (Thomas Swan Carbon Materials Elicarb SW nanotubes, purity 70 - 90%) consisting of SWCNTs with a diameter range 0.9 - 1.7 nm. For the purpose of absorption study at low temperature, the SWCNTs were dispersed in ortho-dichlorobenzene (ODCB) and centrifuged, after which the solvent was let to evaporate to produce a film of SWCNTs on MgF_2 substrate. Another solvent (toluene) and substrate (CaF_2) were tested for assessment of environmental influence. The absorption spectrum revealed that the tubes were not as individuals but rather in bundles. The absorption spectrum was measured between energies 5600 and 8800 cm^{-1} where clear oscillatory structure was observed originating from E_{11} transitions of semiconducting tubes, assessed according to tube diameters and Kataura plot.

Fourier-transform infrared (FTIR) spectra (5600 - 12000 cm-1) with resolution of 4 cm^{-1} were measured with Nicolet Magna-IR 760 spectrometer by using a Quartz beamsplitter and MCT detector. The temperature dependence between 10 - 298 K was measured by placing the sample inside a closed-cycle helium cryostat (ADP Cryogenics) equipped with a resistive heater and a temperature controller. Cryostat was pumped down to ~10^{-7} mbar vacuum with a turbo pump over night. Thermogravimetric analysis was carried out with thermogravimetric analyzer (Perkin-Elmer TGA 7) coupled to a FTIR spectrometer (Perkin Elmer 2000 FTIR). Approximately 6 mg of SWCNT in a Pt cup was heated with temperature ramped between 15 - 850 °C in synthetic air.

3.2   Experiments with fluorescence spectroscopy and microscopy

The studies of emission transitions were performed with raw-material HiPCO SWCNTs gained from Rice University. For PL studies water soluble surfactants form a good environment.[43, 49] Four surfactants were chosen for environmental dependence studies: sodium dodecylbenzenesulfonate (SDBS), sodium taurocholate (STC), sodium cholate (SC) and sodium deoxycholate (SDC) (see Figure 3.1). Surfactants form aggregates around the nanotubes but vary in the type of interaction with nanotube surface and their capability of wrapping the tubes. In SDBS the nanotube is surrounded by hydrocarbon chains forming a micelle around the tube. In cholate-related compounds the cyclohexane structure is non-covalently attached to nanotube wall by π - π stacking interaction. The PL intensities are expected to vary in different surfactants.[43]
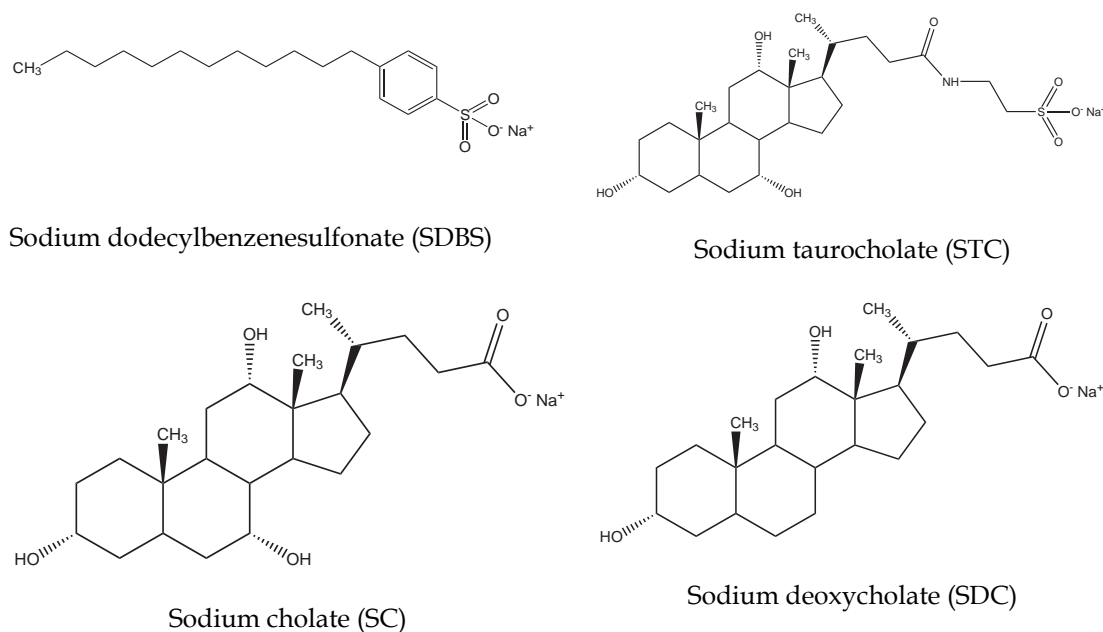
Sodium dodecylbenzenesulfonate (SDBS)

Sodium taurocholate (STC)

Sodium cholate (SC)

Sodium deoxycholate (SDC)

Figure 3.1 Structures of four water soluble surfactants used. SDBS forms a micelle surrounding the nanotube. Cholate-related compounds are attached to nanotube wall by non-covalent π-π interaction.

The samples were ultrasonicated for short period of time and centrifuged to obtain samples containing a fraction of individual SWCNTs with lengths exceeding 2 μm. The dispersions were mixed with melted agarose at 70 ℃ and let cool down as a thin film between microscope slide and cover slip, to immobilize the SWCNTs. The NIR fluorescence imaging and spectroscopy were performed with a custom set up of a modified Nikon TE-2000U microscope equipped with Nikon PlanApo VC 60X/1.4 NA oil-immersion objective.[60] One

output port of the microscope was equipped with a InGaAs near-IR imager (OMA-V 2D, Roper Scientific) and another port was coupled with optical fiber to the entrance slit of spectrograph (Jobin-Yvon C140) with 512 element InGaAs detector array (OMA-V, Roper Scientific). Samples were excited with circularly or linearly polarized continuous wave (cw) diode lasers (λ_{exc} = 659, 730 and 785 nm), tunable cw dye laser and Ti-sapphire laser.

Figure 3.2 Typical image under fluorescence microscope of HiPCO SWCNT. The sample is excited with 659 nm and the nanotube structures with absorption close to resonance are visible with bright PL intensity.
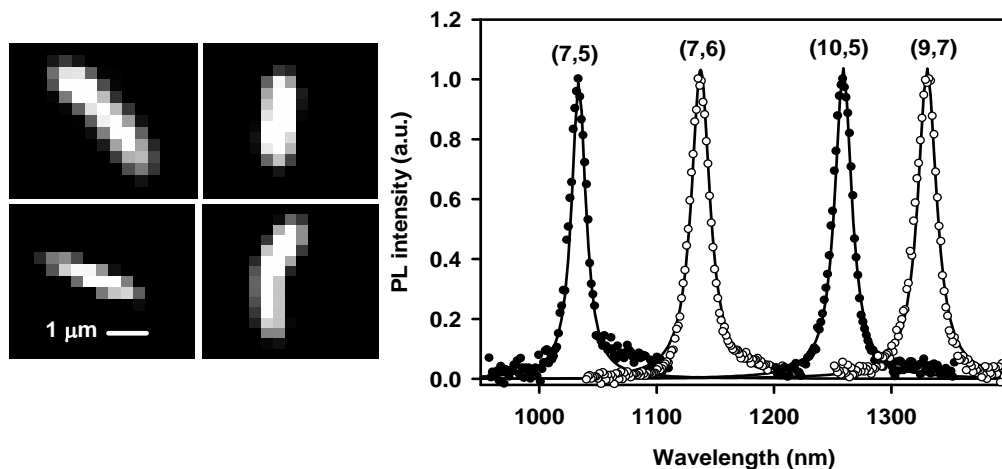
Figure 3.3 Fluorescence images of four individual SWCNTs measured in SDC/agarose and their corresponding emission spectra. Solid lines represent Lorentzian fits. The tubes are identified by comparing the peak positions to the ones measured from PLE map.

In the study of exciton mobilities, the reactant added for PL quenching was an aqueous solution of 4-bromobenzenediazonium tetrafluoroborate (Acros Organics). The diazonium salt forms a covalent bond with SWCNTs. [73] SDC was chosen to be used for other PL measurements, since it produces the

highest PL intensity. Highly significant part of the measurements is the selection and identification of nanotubes which would represent nearly pristine SWCNTs with only little defects. When searching the nanotubes under the fluorescence microscope, only the most intense ones were chosen for spectral analysis (see Figure 3.2). These are likely to represent nanotubes with E_{22} absorption transition close to the excitation wavelength. For each diode laser there are four nanotube structures that have close resonance absorption transitions. The tuneable lasers were adjusted explicitly for certain nanotube resonance wavelength. SWCNTs were characterized by comparing PL spectrum of the individual tube to the structure assigned PLE map[1] measured from ensemble sample. (see Figure 3.3). After characterising the tube, the following criteria were used to select nanotubes: length greater than 2 µm to minimize the influence of end-related quenching effects, absence of defects seen as non-uniformities in SWNCT spatial emission profile, and emission peak maxima within 3 nm from the average ensemble E_{11} emission maxima as found in the bulk samples. Also the stability of PL intensity needed to be evaluated. This turned out to be important, since detailed observation revealed that most tubes are not stable, but show PL quenching as well-defined steps or rapid fluctuations, "jumping". PL intensities were measured for each nanotube structure with same measurement set up to make them comparable to each other. The excitation power and focusing were taken under consideration. The experimental excitation intensities were normalised by the number of carbon atoms and scaled down by a relation $\sigma(\lambda_{22})/ \sigma(\lambda_{exc})$ where $\sigma(\lambda_{22})$ and $\sigma(\lambda_{exc})$ are absorption cross-sections at the E_{22} resonance and the excitation wavelength, respectively, obtained from bulk PLE maps of SWCNT suspension.[34]

For study of exciton dynamics six nanotube structures were chosen: (10,2), (9,5), (8,6), (8,7), (10,5) and (9,7). The same criteria and procedure were used for identification and selection of tubes as previously. The fluorescence images where measured time-resolved with 50 ms frames, ~10 s for each with excitation power attenuated by a set of filters, measured from low to high intensity and back between. The excitation power was varied between 0.02 and 100 kW/cm^2 with a focused laser spot. The importance of measuring time-resolved PL was again demonstrated since significant part of the measured nanotubes did not have stable PL intensity even at relatively low excitation levels. If only accumulation had been collected, the tubes having various types of fluctuation behavior, stepwise or just "jumping" could not have been observed.

4 RESULTS AND DISCUSSION

4.1 Temperature dependence of excitonic absorption

For the purpose of light emitting applications of carbon nanotubes, the processes occurring after photoexcitation are of high interest. However, to fully understand these processes, and especially environmental and structural dependencies, it is useful to also study the absorption. The importance of this study lies in the complexity of the environmentally induced mechanisms to alter the energy gap and shift the electronic absorption transitions as a function of temperature. Most of the temperature dependence studies have been done with Raman[74-77] and PL spectroscopy[31, 78], while in this study the electronic absorption spectroscopy was used.

As shown in Figure 4.1, the baseline corrected NIR-absorption spectra at three temperatures illustrate obvious sharpening of peaks at lower temperatures. The peaks are suggested to originate from the E_{11} transitions of SWCNTs that are bundled and in contact with the surface, and thus cannot be assigned according to Bachilo et al.[1] The spectra are fitted with multi-Gaussian function clearly distinguishable at 10 K. Since the bandwidths are hampered by removal of continuum baseline and to some extent, overlapping of peaks, the most reliable information about temperature dependence is gained from peak positions that are more accurately determined. The temperature dependencies show three type of behavior in increasing temperature: blueshift (peaks 1 - 3), redshift (peak 4) and no shift (peak 5) within error limits (see Figure 4.2). Most interesting are the peaks 1 and 2 that show smooth blueshift between 10 and 175 K and then very abrupt blueshift at ~200 K (see Figure 4.3). The temperature effect on band positions is reversible without hysteresis.
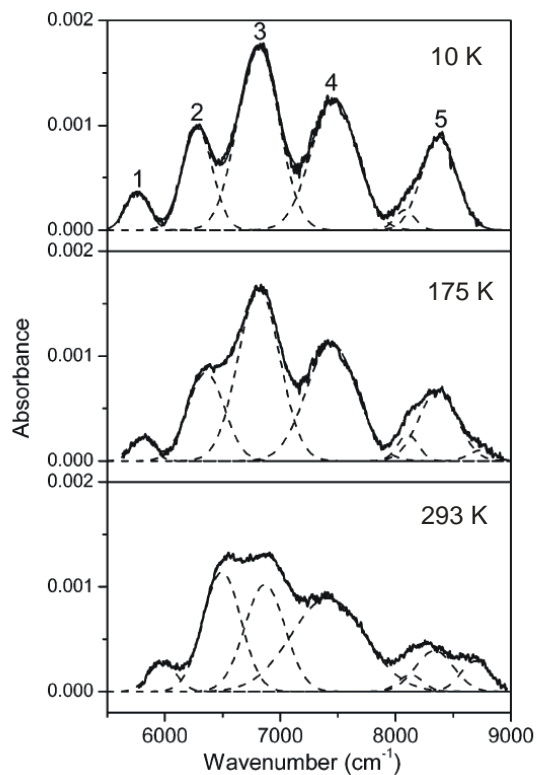
Figure 4.1 Baseline corrected NIR absorption spectrum of SWCNT film at 10 K, 175 K and 293 K. The spectra are fitted with multi-Gaussian represented with dashed lines. The bands 1 - 3 blueshift and band 4 redshifts. Band 5 does not shift within error limits.
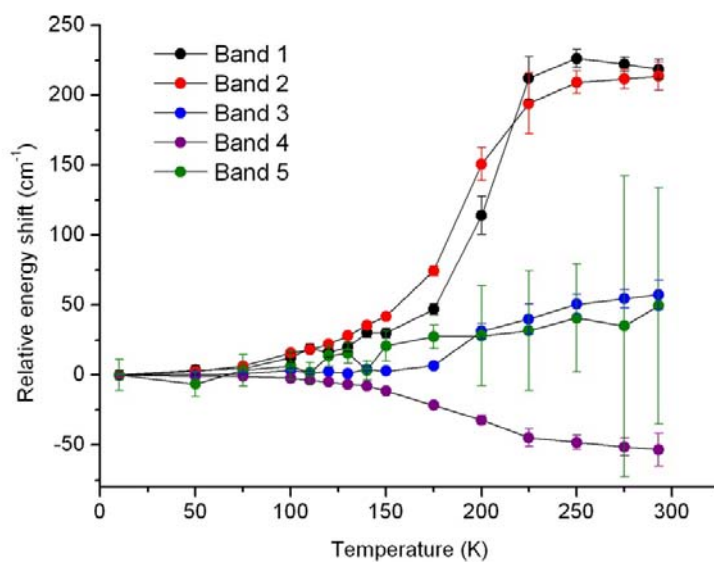

Figure 4.2 The relative energy shifts as a function of temperature. Bands 1, 2 and 3 blueshift, whereas band 4 slightly redshifts and band 5 does not shift within error limits.
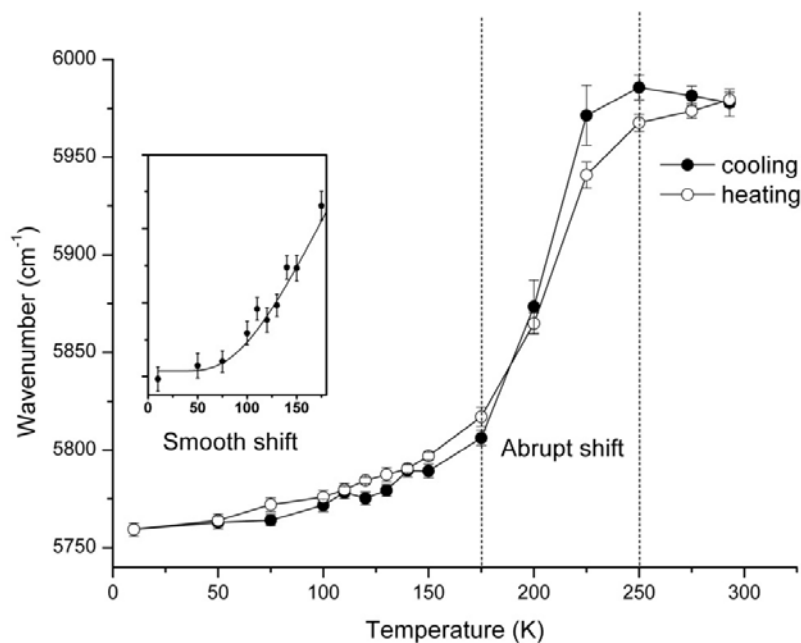
Figure 4.3 The transition energy shift of band 1 as a function of temperature for a cooling cycle (filled circle) and for a heating cycle (open circle). Between 10 and 175 K the shift is smooth and can be described with Bose-Einstein statistics (inset). Around 200 K, the shift is abrupt and saturates >250 K.

The analysis can be divided according to these two temperature ranges. At 10 - 175 K, the data is fitted with equation describing Bose-Einstein statistics for thermal population of phonons (Equation 1, Article I Correction). The Bose-Einstein fitting can provide understanding of coupling between phonons and excitonic state. The phonon frequency values obtained correspond to typical RBM frequencies and are in agreement with previous studies.[78] An interesting question arises from the sign of the shift. The band gap shift due to electron-phonon coupling is expected to be negative[54, 55] whereas our study indicates both positive and negative shift. Differences in thermal expansion coefficients can cause mechanical strain along nanotube and alter the electronic structure. The most prominent causes of strain are tubes themselves inside bundles and the substrate where the film is dried on. The latter option was tested with two different substrates and it was concluded that significant difference in thermal expansion coefficient did hardly change the shift. Then again the bundling might not be good enough explanation for such a smooth shift. Since the bundles are formed without any structure preference, the transition peak should be strongly broadened rather than shifted. The possible explanation could lie in the presence of other substance adsorbed on nanotubes. Since the sample was kept under high vacuum conditions (~10^{-7} mbar), the only prominent option really is water. At this point we can also consider the second

part of analysis, abrupt shifts around 200 K most likely to be caused by strong environmental change.

It is very difficult to remove water vapor even in vacuum, due to its low vapor pressure and its remarkable capability to interact with surfaces via hydrogen bonding. Even extensive pumping in high vacuum is not enough to extract all water. This is why it is reasonable to assume that our sample contains some amount of water. There are a couple of options to explain the phenomena under investigation. One option is adsorption/desorption of water vapor. This was further investigated with thermogravimetry coupled with FTIR. The results indicate that some water is released upon heating from bulk nanotube sample. However more accurate analysis is impossible due to small mass of the analyzed sample. The water detected in FTIR rises smoothly up to even 850 °C, suggesting that water is first desorbed from tubes but adsorbed onto the walls of the system, and released later. However, further tests made to support adsorption/desorption of water onto the walls of nanotubes did not turn out as expected. Shortly, the sample film was measured and cooled to 10 K, then heated over night at ~300 °C, measured again and finally exposed to water vapor at room temperature for 2 days and measured again. There was a clear difference between the spectra of the original and heated sample, but interestingly, the spectra of vapor treated sample did not return to the original one. This suggests that sufficient amount of water is not adsorbed to nanotubes under these conditions to reversibly change the spectrum back to original. This led us to discuss another alternative: strain caused by water trapped inside the nanotube. Theoretical studies suggest that water could form a 'nanotube' when trapped and confined inside a nanotube.[79] The theory is supported by a research by X-ray diffraction.[80] The phase transition temperature can depend on the tube diameter.[79, 81] The phase transition of water nanotube inside SWCNTs could be the most prominent explanation for our observations. Since the electronic structure of SWCNT is highly sensitive to the environment, it can be expected that the strong shift is caused by phase transition of water. The temperature for phase transition of structured water can be expected to be higher than for adsorbed water, which could explain the strong shift at ~200 K and is in accordance with previous result.[80] In addition, the water trapped inside the nanotube could explain our experiment with heating and adsorbing water back again. It is possible that water is released upon heating but cannot be condensed inside the tube again in water vapor conditions. The suggested process is that water has been trapped inside the nanotube during wet processes done for purification of the samples, generally including ultrasonication treatments with aqueous acids.

Though the idea of water nanotube inside SWCNT could explain our observation, our method is not sensitive enough to validate this suggestion. The certain conclusion to be made is that the temperature shifts are caused by environment, most prominently water. The suggested mechanisms are adsorption/desorption of water and strain caused by phase transition of water confined inside the nanotube. The crucial problem in this study, as in many

other SWCNT studies, was the sample itself. For studies of electron-phonon coupling, it would be useful to study individual SWCNTs. The absorbance measurement of individual tube is extremely challenging due to low intensity and could not have been achieved in this work. However, this study indicates the importance of the temperature effect, which should be taken into consideration when analyzing   experimental results against theoretical predictions.

4.2 Exciton mobility

After realization that semiconducting SWCNTs create bound excitons rather than free charge carriers, the size and mobility of excitons has been under intensive research. The exciton mobility is important for understanding linear and non-linear optical responses. Exciton motion is closely related to properties like PL quantum yield and exciton lifetime. The noticeable mobility of excitons makes PL intensity highly sensitive to quenching sites that can be intrinsic defects or environmentally created sites as a result of processes such as oxidation or functionalization. Cognet et al.[23] studied exciton mobility with single-molecule chemical reactions with individual SWCNTs and discovered that oxidation or functionalization causes the PL intensity to quench in steps. Analysis of the step size against initial PL intensity in SDBS revealed that exciton range Λ, the distance traveled by the exciton during its lifetime, was ~90 nm. The nature of exciton motion has been predicted to be diffusional with diffusion coefficient D 0.1 - 0.4 cm^2 s^{-1}.[21, 23] In this research an attempt was made for measuring the exciton range Λ in different environments for a single (n,m) species.

Movies with 50 ms frames of an individual SWCNT under fluorescence microscope were recorded after addition of the quenching salt, 4-bromobenzenediazonium tetrafluoroborate (see Figure 4.4). The diazonium salt reacts with SWCNT forming a covalent bond. The single-molecule reaction events were observed as drops in PL intensity at the reaction site. Differential image sequences of n frames between n-1 and n+1 frame revealed that the chemical reaction events were apparent as spatially localized, diffraction limited peaks centered on nanotube axis. These reaction events are visible as distinct steps in time-dependent PL intensity. The size of chemical reaction sites in our measurement are below the diffraction limit, which is approximately ~1 μm (~3 pixel area). The exciton range (Λ) cannot be measured directly, but can be calculated with equation

$$\Lambda = \frac{\Delta}{I/L}$$
<div align="right">Equation 4.1</div>

where Δ is the magnitude of the intensity drop and I/L is the initial intensity per unit of length (see Figure 4.4).
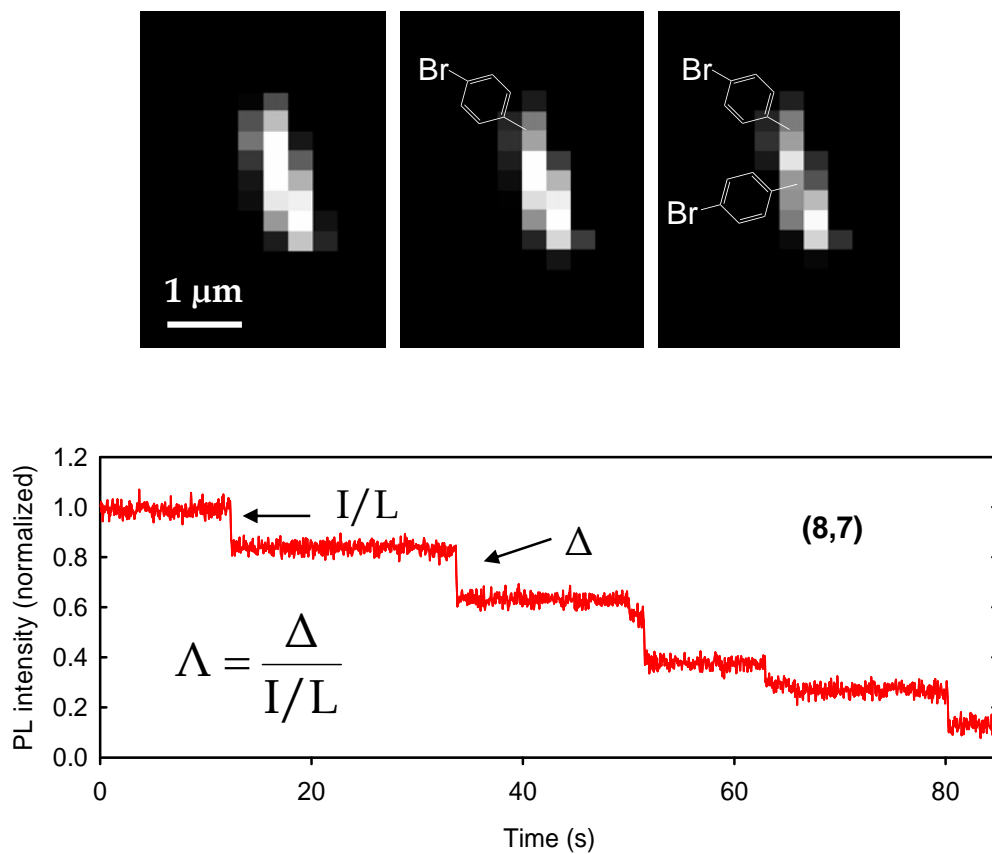
Figure 4.4 Near-IR fluorescence image of an individual (8,7) nanotube suspended in SDC (up left). The single-molecule reactions with diazonium salt are observed as quenched spots (up middle and right). Time-dependent fluorescence intensity of the nanotube after addition of reactant (below).

To be able to distinguish between Λ values in different environments, a Matlab algorithm was developed for the analysis. The program was designed to identify reaction events from the frame sequence and to evaluate the intensity change of reaction event with 2-dimensional Gaussian fitting. A common complication in this procedure is visible in the time-dependent PL intensity (see Figure 4.4) as the step amplitudes decrease in the course of the reaction. This is expected as the already existing quenching sites effect the PL intensity. The first obvious option would be to compare the intensity drop to the level right before the reaction event, as the interest is in the relative change of PL intensity. Unfortunately the determination of this intensity level did not prove to be reliable, because of interference of existing defects.
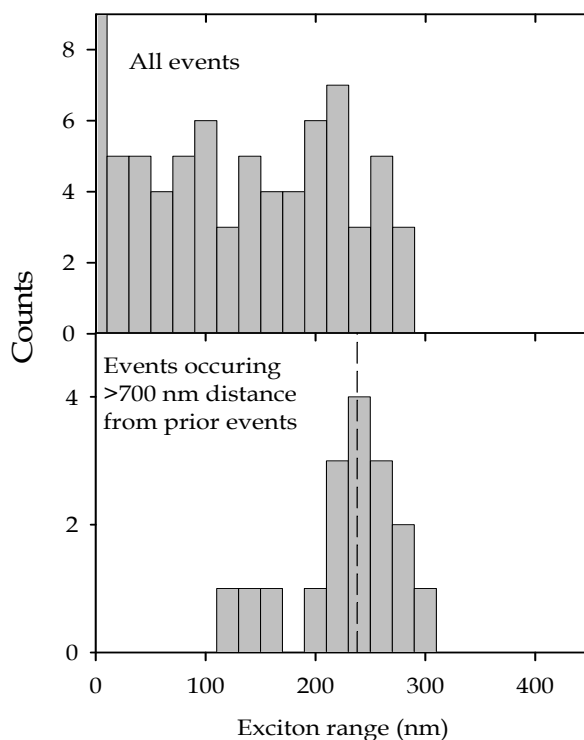
Figure 4.5 Histograms of the measured exciton ranges, Λ, for (7,5) SWCNTs in SDC. The upper histogram represents all data points received after algorithm. The lower histogram represents data where events closer than 700 nm distance from prior events are removed. The dashed vertical line indicates an average value of 238 nm. The bins are 20 nm.

Figure 4.6 Position/time map for the steps labeled in order of appearance, with symbol diameters proportional to the step magnitudes. This map shows that the largest step events tend to occur at early times and are spatially separated from each other.

The evaluation of the most reliable data points proved to be the most difficult and challenging part of this work. The following path was taken when estimating the most 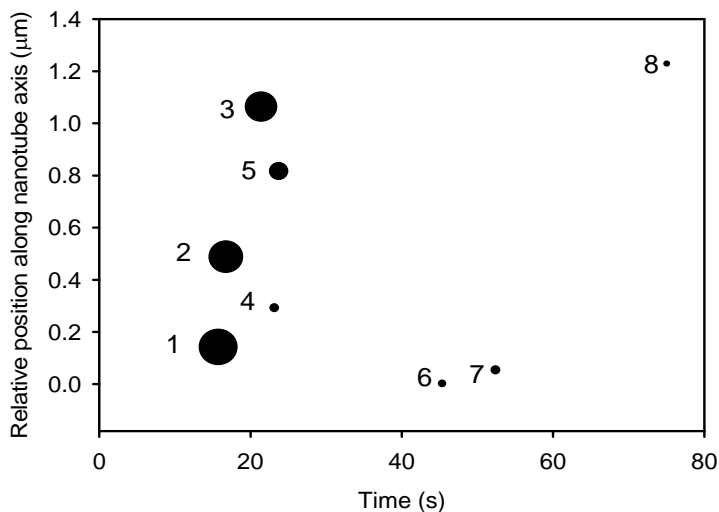reliable exciton range for (*7,5*) structure in SDC. The data is collected from 10 individual tubes. More than 20 tubes were measured altogether, but after careful analysis of the stability of the PL intensity and also the stability of physical position, some of them were rejected. Histogram including all reaction events (see Figure 4.5) indicates largest contribution around 220 nm and then noticeable amount of events at shorter exciton ranges, arising from chemical attacks at a site close enough to a previously formed quenching site resulting in diminished intensity of steps. The 0-bar is arising from artificial data points. This was justified with step intensity versus time profile indicating a pattern of decreasing intensity (see Figure 4.6) Only those events that are spatially well separated from prior quenching sites provide reliable data for the determination of Λ; others were discarded. To implement this restriction, we computed the distance between each new quenching site and all prior quenching sites on the same nanotube. Any intensity steps located within 700 nm of a prior event site are excluded from the compilation of Λ values. This allows only ~5 % spatial overlap between sequencing steps. In the final round of the analysis, these points were excluded resulting exciton range of 238 ± 24 nm (see Figure 4.5). This value was estimated as the most reliable exciton range, and it is consistent with the value gained with the two other iterations. The values for (*7,5*) in other surfactants were 144 ± 26 nm in SDBS, 182 ± 18 nm in STC and 178 ± 20 nm in SC. The quoted experimental uncertainties equal twice the standard error of the mean. The value in SDBS is somewhat higher than estimated in a previous study.[23] In this study special attention was paid on the quality of the tubes to make sure that most pristine tubes were represented. In previous study some of the steps were possibly falsely judged as double or triple events occurring within a diffraction limited area. As the diazonium salt concentration was kept low, the events are well separated in time and space as observed in time-dependent PL intensity (see Figure 4.6), the probability of multiple events should be negligible. The intensity of a step was also estimated more precisely with Gaussian fitting. A recent work with air-suspended SWCNTs reported substantially longer exciton range, above 600 nm, as can be expected.[82]
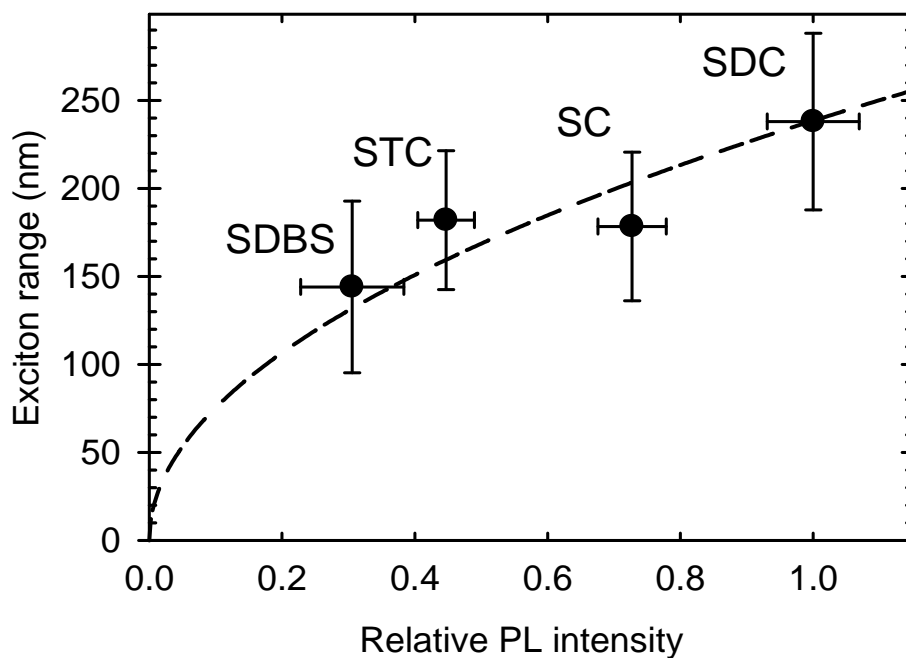
Figure 4.7 Exciton range, Λ, of (7,5) SWNCTs as a function of the relative PL intensity per carbon atom (*I*) for four different surfactant environments. Error bars show standard deviations of data sets. The dashed curve is the best least-squares fit to the function $a\sqrt{I}$.

To understand the environmental effects observed in exciton mobility it is necessary to correlate the results with another photophysical property, i.e. the PL action cross-section, 'brightness' or relative PL intensity. This parameter is known to depend significantly on SWCNT environment. [34, 43, 45, 83] The PL action cross-section is the product of absorption cross-section at the E_{22} transition maximum ($\sigma(\lambda_{22})$) and the PL quantum yield (Φ_{PL}), $\sigma(\lambda_{22}) \times \Phi_{PL}$. The relative action cross-sections that are proportional to relative intensities were measured independently for (7,5) in SDBS, STC, SC and SDC. The correlation between exciton range and PL intensities relative to action cross-section shows obvious monotonic relation (see Figure 4.7). The environment dependent variation is attributed mainly to different quantum yields, because E_{22} spectral transitions are weakly dependent on environment. Assuming that E_{11} radiative rate is also relatively constant, the PL intensities can be considered to be proportional to the exciton lifetime τ. The correlation observed in Figure 4.7 is consistent with a square root dependence, indicating that exciton range is proportional to $\sqrt{\tau}$. According to the law of diffusion distance traveled by a particle is proportional to $\sqrt{D\tau}$, where D is the diffusion coefficient. The result strongly supports the view of localized excitons with substantial diffusional motion along tube axis. Here it should be noted that D might be surfactant dependent, but the dependence has not been studied. The main contributor to the differences in exciton ranges is considered to be the exciton lifetime, which is known to be

surfactant dependent. Duque et al. reported that exciton lifetimes measured from individual (6,5) tubes are approximately four times longer in SDC than in SDBS.[45]
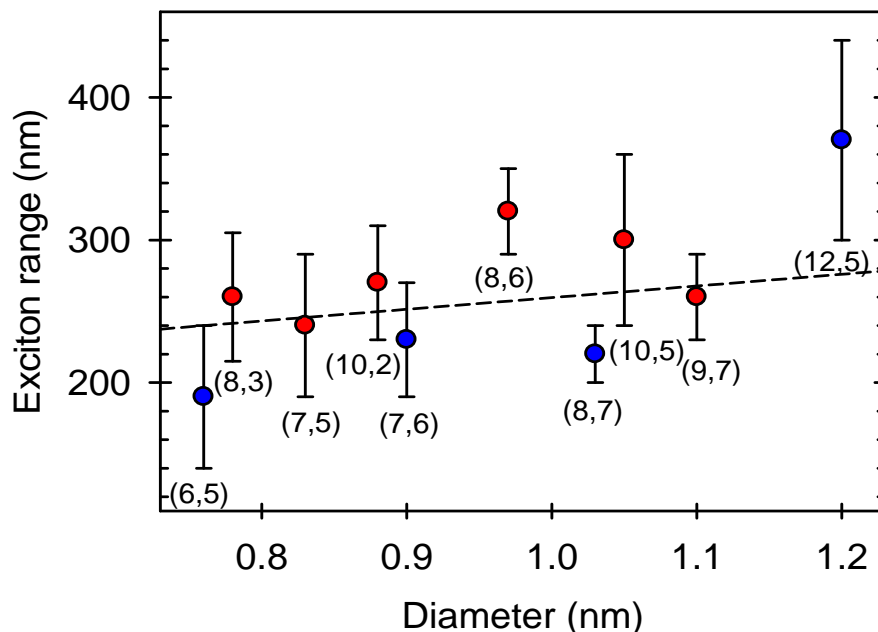

Figure 4.8 Diameter dependence of exciton range for ten (*n,m*) structures. The Mod 1 and Mod 2 are indicated with blue and red, respectively. The dashed line is a statistically weighted linear best fit to the data.

The study of environmental dependence of exciton mobility was performed with (7,5) tubes to eliminate any variation originating from (*n,m*) structure. However, many optical properties can be expected to vary according to structure such as PL quantum yield Φ_{PL}, absorption cross-section $\sigma(\lambda_{22})$, diffusion coefficient D, exciton lifetime and relaxation rate from E_{22} to E_{11}. This is why it is of high interest to study structure-dependence of exciton ranges. The measurements and analysis were performed using SDC as the surfactant. Figure 4.8 shows the exciton ranges for 10 nanotube structures as a function of diameter. The values vary between 190 - 370 nm with a weak positive correlation. No clear difference in exciton ranges between mod 1 and mod 2 groups is observed.

The PL action cross-section, which is proportional to PL intensity, is known to have strong structure dependence (see Figure 4.9). The general trend observed is that larger diameter structures emit at lower energy level with lower PL intensity. The observed difference within the measured 10 structures is a factor of six, where (10,2) is the brightest and (9,7) and (12,5) the dimmest.

The tube (10,2) has been predicted to be the brightest in theoretical work[26] and in measurements performed in SDBS[34]. The exciton ranges for a single structure in various surfactants showed a difference of 100 nm while PL changed by a factor of three. One could expect a similar trend for structure-dependence. However, the exciton range does not show strong correlation with the PL intensity for different (n,m) (see Figure 4.10). Statistically weighted linear best fit to the data shows a slope not significantly different from zero. The PL intensity on x-axis is proportional to $\sigma(\lambda_{22}) \times \Phi_{PL}$, where Φ_{PL} is proportional to exciton lifetime τ and exciton non-radiative relaxation rate from the initial (E_{22}) to the emitting (E_{11}) excitonic state. According to our exciton diffusion results, the y-axis is proportional to $\sqrt{D\tau}$. All the parameters mentioned here are likely to have structure dependence, but the sign and strength of the structure-dependence are not yet defined. It is possible that D and τ, for example, have opposing effects so that their product remains nearly constant. More probable explanation could be that the strong structure-dependence of PL action cross-section is not originating from τ, but from absorption cross-section. Theoretical study by Oyama et al. suggested a strong decreasing trend in absorption intensity within families with same $2n-m$ value.[26] However, at the moment there is no conclusive experimental data on structure-dependence of absorption cross-section which could support our observation.
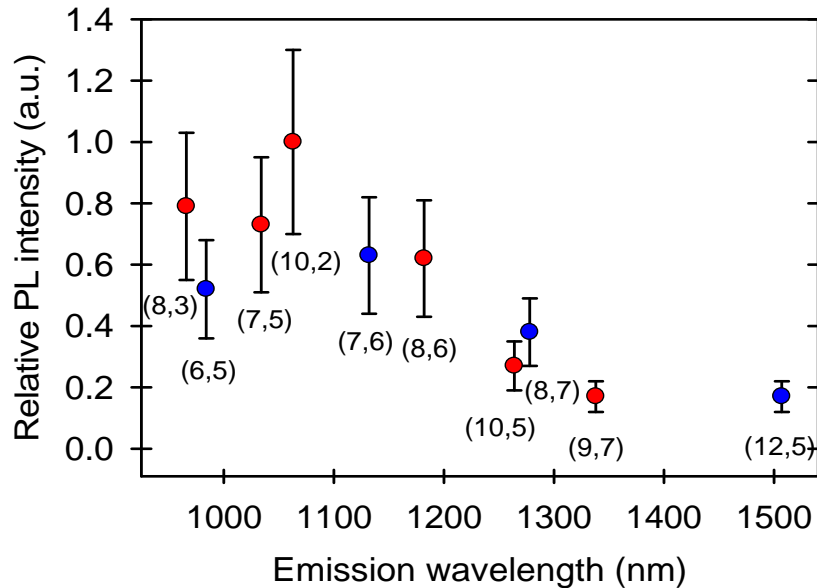

Figure 4.9 Relative PL intensity as a function of emission wavelength for ten (n,m) structures. PL intensity has clear structure-dependence. The Mod 1 and Mod 2 are indicated with blue and red, respectively.
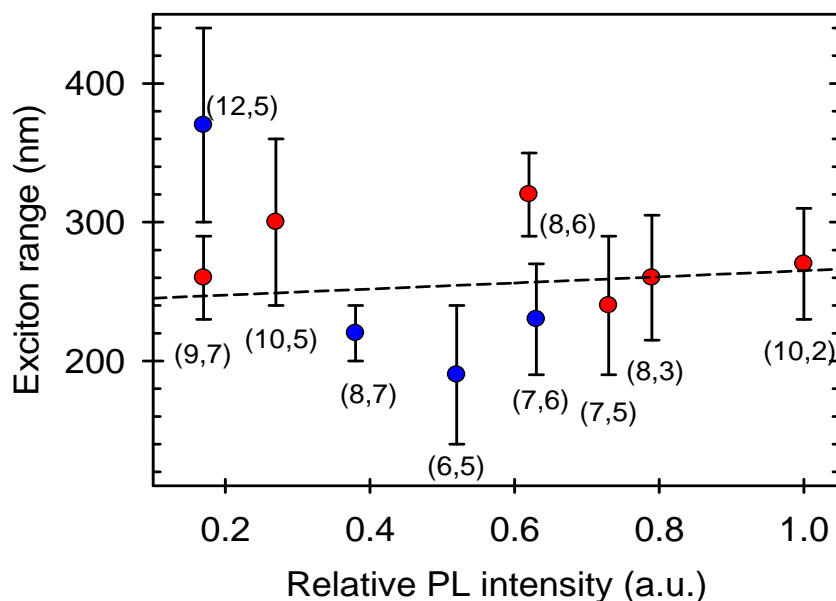
Figure 4.10 Exciton range as a function of relative PL intensity. The dashed line is a statistically weighted linear best fit to the data; its slope is not significantly different from zero. The Mod 1 and Mod 2 are indicated with blue and red, respectively.

The results presented here directly show that exciton mobility has dependence on environment and PL dependence supports the model of localized excitons having substantial diffusional mobility along nanotube axis. With exciton lifetime of 50 to 300 ps[24, 45] the diffusion coefficient D is estimated to be between 0.2 and 2.8 cm^2 s^{-1}, in the same range as reported in prior studies.[21, 23] With proof of diffusional motion, exciton lifetimes and exciton ranges can be connected via diffusion law. Understanding the nature of exciton mobility is important for prospective use of SWCNTs in optoelectronics. Because of substantial exciton mobility, PL intensity is highly sensitive to chemical derivatizations and protonation. Because of this property, the use of SWCNTs as fluorescent nanosensors for detection of single molecules is promising. The advantage of surfactant/water environment used in this study is that it could be appropriate for biological applications. The complications encountered during measurements and data analysis support the sensitivity of SWCNT electronical structure to extrinsic effects: only a small proportion of characterized SWCNTs was stable enough for analysis. It also explains the difficulty of comparing the results obtained from ensemble samples against individual tubes. The percentage of nearly pristine tubes is low and ensemble measurements are hampered by damaged material.

4.3 Exciton dynamics

Since the excitons in SWCNT have notable mobility along the nanotube axis, it is predicted that when exciting with sufficiently high excitation powers, the increased number of excitons would lead to substantial interactions. Studies of exciton-exciton interaction (EEA) processes are needed for understanding exciton dynamics. Interactions are observed as nonlinearity in PL intensity at higher excitation levels, whereas PL intensity is linearly proportional to excitation intensity at low levels. Our approach was to study nonlinearity of individual SWCNTs under continuous laser excitation in SDC.
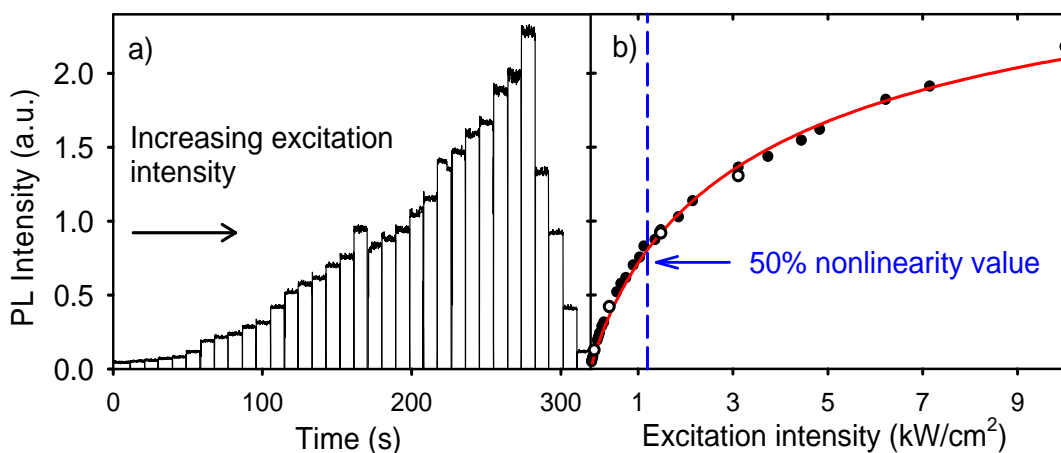

Figure 4.11 PL intensity measurements on an individual (10,5) SWCNT. In a), each bar shows repeated 50 ms intensity measurements at a single excitation level that is adjusted from bar to bar. In b) the average of each PL intensity bar is calculated and plotted versus excitation intensity. Closed circles indicate measurements taken at increasing excitation intensity; open circles show values for decreasing intensity. The process is reversible. The smooth red curve shows a fit by equation describing the experimental data. The dashed blue vertical line marks the intensity giving 50 % nonlinearity.

The emission was collected from ~1 µm² area positioned at maximum intensity and averaged to visualize the nonlinearity (see Figure 4.11). The PL increase is linear below 0.5 kW/cm² after which apparent nonlinearity is observed. The nanotube represented in Figure 4.11 has stable PL throughout the measurement and the data points measured with increasing and decreasing intensity show good repeatability, indicating that no permanent photoinduced change in emissive behavior is present. Only approximately half of the measured nanotubes displayed such smooth and reversible excitation dependence. To compare the magnitude of nonlinearity, the experimental traces

were fitted with non-physical function and intensity at point where PL signal relative to excitation intensity is quenched by a factor 2, I_{50}, was recorded. The I_{50} dependence against the relative PL intensity indicates that "dimmer" tubes have generally higher nonlinearity threshold (see Figure 4.12). The potential explanations for high threshold can be 1) shorter exciton lifetime providing less time for interaction and 2) smaller absorption cross-section value, meaning decreased absorption probability and exciton density. The lack of structure dependence in exciton diffusion ranges suggests that absorption cross-section is more likely explanation. On the other hand, to evaluate the effect of exciton lifetime on the saturation value, (10,2) was measured additionally in SDBS. The PL intensity of (10,2) in SDBS is approximately five times less than in SDC. Since the absorption cross-section is the same, the difference arises mainly from exciton lifetimes. The observation coincides well with the differences observed in measured exciton lifetimes.[45] The results indicated clearly higher I_{50} in SDBS, which is in agreement with exciton lifetimes and diffusional range.
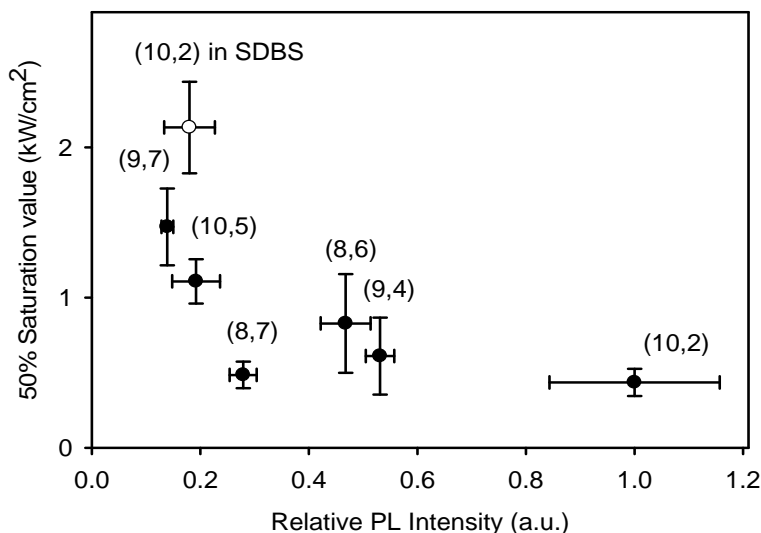
Figure 4.12 50 % Saturation value of six different nanotube structures as a function of relative PL intensity. The measurements are done in SDC surfactant (solid circle) and additionally (10, 2) is measured in SDBS (open circle). Error bars show standard deviation of the datasets.

The early studies of nonlinearity in bulk samples attributed the nonlinearity to Auger-type exciton-exciton annihilation (EEA).[20, 42] However, recent studies utilizing ultra-fast spectroscopy[25] and continuous wave spectroscopy[24] indicate that PL nonlinearity appears in such a low intensity regime that nonlinearity cannot be explained by EEA. Non-linearity study of individual tubes under pulsed laser excitation indicated that EEA is highly efficient, and saturation is observed with 2 - 6 excitons per some micrometers.[25] However, in our study the lowest I_{50} value for (10,2) is ~0.4 kW/cm². Assuming SWCNT absorption cross-section $\sigma(\lambda_{22})$ of 10^{-12} cm²/µm[24, 25] and intrinsic exciton

lifetime less than 100 ps (major component) [24, 45] the average number of photons absorbed by a 1 μm segment of nanotube during exciton lifetime equals ~0.2. Considering the exciton diffusion ranges 230 nm, the exciton concentration is far too low to explain quenching of 50% at this excitation level. However, since the exciton lifetimes are not yet well defined it is not possible to disregard this mechanism.

The exciton population n at E_{11} energy level can be described with equation

$$\frac{dN}{dt} = \sigma(\lambda_{22}) \cdot I_{exc} - k_1 \cdot N - k_2(N) \cdot N^2 \qquad \text{Equation 4.2}$$

where k_1 is the internal decay rate of exciton and $k_2(N)$ is the rate coefficient of EEA. For 1D situation, $k_2(N)$ is not a constant but depends significantly on the average distance between excitons and fluctuates in time.[84] Thus, the equation does not have an analytical solution. To further study our experimental results within the model of EEA we performed numerical simulation to model one-dimensional diffusion of excitons. Excitons are randomly created along the nanotube with given absorption cross-section, 10^{-12} cm²/μm and increasing excitation intensity. The excitons moved along the tube with small steps δ (describing exciton size) during elementary time Δt, defining the simulated diffusion coefficient D. Upon collision with each other one of the excitons is quenched. The PL intensity is given by average exciton population density. The length of the tube is set long enough to avoid end-related quenching and exciton size δ $<< \sqrt{D\tau}$. The excitation intensity was varied by five orders of magnitude which produced highly non-linear curves reaching nearly PL saturation.

The significant parameter in EEA process is the distance between excitons, which is described with Λ. Simulated curves with arbitrary k_1 and D but with the same Λ are similar, transformed one into another by appropriate scaling of excitation intensity coordinate. Internal decay rate k_1 for exciton is set so that condition $2\sqrt{D/k_1} = \Lambda$ is satisfied with average exciton range Λ = 260 nm. This allows us to compare experimental and simulated traces by scaling. The simulated trace is fitted to an experimental trace to find scaling factors for x- and y-axis, c_x and c_y. The y-coordinate, PL intensity, is dependent on parameters of action cross-section and experimental detection efficiency and could be fixed once these parameters are well defined. However, in this experiment they were allowed to vary according to the best possible fit.

The simulated trace fits the experimental trace very well indicating that the model of EEA can describe our experimental nonlinearity processes (see Figure 4.13). Due to the similarity, the experimental decay rate and diffusion coefficient can be calculated as $c_x \cdot k_1$ and $c_x \cdot D$. The results of diffusion coefficient and exciton lifetime $(k_1)^{-1}$ according to the model that attributes all nonlinearity to EEA imply that exciton lifetimes are on the order of several nanoseconds. The

reported exciton lifetimes are far shorter, 50 - 100 ps.[24, 45] The unrealistically long exciton lifetimes strongly imply that EEA is not the only process attributing to the observed nonlinearity and other long lived quenching species are relevant.
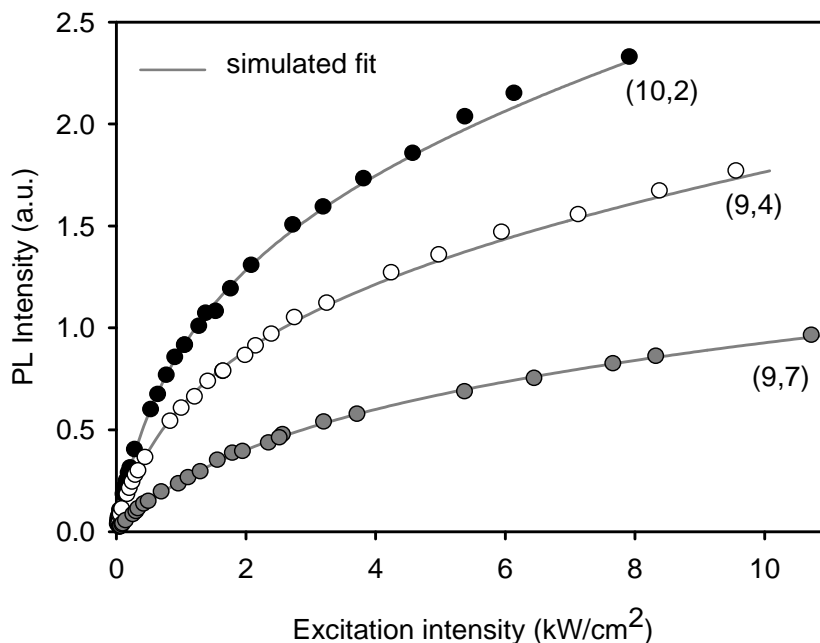

Figure 4.13 Experimental nonlinearity (circles) of three SWCNT structures with scaled fit from model simulations.

The possible presence of metastable quenching states needs to be discussed. The model described here can be extended to include a small fraction of the exciton population converted into metastable states X. The decay rate constant k_1 will be replaced by $k_1 + k_X$ and EEA rate constant $k_2(N)$ will become

$k_2(N) + k_2(N, X)\dfrac{k_x}{k_{1X}}$ for Equation 4.2 when population of quenchers is

proportional to the population of excitons. Here k_x describes the rate constant for exciton conversion to metastable species X and k_{1x} is the first-order rate constant for decay of X species. The modified kinetics equation imply that the population of X is related to the population of excitons by a factor of k_x/k_{1x}, and metastable species X can be the dominant quencher at high excitation intensities.

The character of the long-lived quencher remains to be revealed. The presence of long-lived dark states has been proven experimentally[32, 33] and discussed in theory[27-29]. Possible candidates are dark singlet or triplet state excitons or separated charge carriers formed by exciton dissociation. Our test with frequency modulated excitation light indicates that the lifetimes of these

long-lived quenching states are less than 1 ms. Some evidence of light-induced quenching states was observed. A test with two different low levels of excitation was performed, so that the excitation intensity corresponded to linear and early non-linear excitation level. At linear regime excitation, no distinct fluctuations in SWCNT PL were observed. At nonlinear regime many distinct reversible steps lasting ~0,1 to 10 s were observed. Qualitatively similar PL quenching has been observed by protonation and deprotonation.[23] The possible source in our measurement could be photo-assisted protonation or charge separation. In addition, similar excitation dependence studies were performed with excitation higher by factor of ten. The observations of gradually decreasing PL after increased excitation and slow increase after decrease in excitation support quencher generated by light exposure.

The results suggest that experimental nonlinear quenching of SWCNTs is well described by EEA process, but with unrealistically long exciton lifetime. This indicates that nonlinearity is not merely originating from EEA, but fraction of excitons is converted into photoinduced metastable quenching species. Such PL quenching states could be dark singlet excitons, triple excitons or charge separated states, with lifetimes less than 1 ms. In some cases we also observed reversible photoinduced PL quenching with times up to 10 s. The possible sources of such steps could be arising from charge separation induced by EEA or photo-assisted protonation.

5   SUMMARY AND CONCLUSIONS

In the work presented in this thesis, optical properties of single-walled carbon nanotubes were studied experimentally with FTIR absorption spectroscopy and fluorescence spectroscopy and microscopy. Though the full understanding of the complex nature of SWCNT photophysical processes involving excitons was not yet revealed, some significant steps were made.

The study of temperature dependence of excitonic absorptions demonstrates that absorption processes are sensitive to both intrinsic and extrinsic factors.   The intrinsic effect observed was a smooth energy shift between 10 and 175 K and was interpreted to arise from coupling between excitonic state and possibly RBM phonons. Even stronger energy shift was originating from extrinsic factor. An abrupt blueshift observed at 175 – 250 K was interpreted to arise from interactions with water. Interesting plausible explanation could be strain caused by confined water trapped inside SWCNTs.

In the study of exciton mobility, exciton ranges Λ were defined for different (n,m) structures and in different environments. The large values (140 - 340 nm) explain well the sensitivity of SWCNT PL to chances in local environment. The results indicated that Λ is substantially dependent on surrounding surfactant but not dependent on (n,m) structure. The observed positive correlation between Λ and PL intensity support the view of localized exciton with noticeable diffusional motion along the nanotube axis. The lack of structure dependence of Λ compared with strong structural dependence of PL action cross-section revealed an unexpected and interesting observation. The result could imply that the dominating factor in PL action cross-section is in fact absorption cross-section. The studies on exciton mobility reported in this thesis will be useful when reliable measurements of absorption cross-section and exciton lifetimes for different (n,m) structures are achieved.

The studies of exciton dynamics indicated that nonlinearity regime of PL is observed at such low excitation intensities that exciton-exciton annihilation reactions should be negligible. The suggested explanation involves conversion of excitonic states into photoinduced metastable quenching states, that could be dark singlet or triplet states or charge separated states. Further studies are

needed to confirm the extent and nature of these states. Important part of the work done here involved the development of simple method involving comparison of experimental and theoretical nonlinearities. When for example reliable exciton lifetimes are revealed, the method can be used for analyzing the proportional population and conversion rate for metastable quenching states X.

A general feature connecting all studies performed is the sensitivity of SWCNTs towards the environment. For avoiding problems arising from the sensitivity and on the other hand exploiting the opportunities it offers, the study of SWCNT interactions with environment needs to be further studied theoretically and experimentally. Studying individual SWCNTs is a key technique for truly understanding processes involving optical properties and their structure dependence. However, many potential applications require controlled manipulation of ensemble SWCNTs, which can be enabled by good understanding of SWCNT interactions with surrounding molecules.

REFERENCES

1. S. M. Bachilo, M. S. Strano, C. Kittrell, R. H. Hauge, R. E. Smalley and R. B. Weisman, Structure-Assigned Optical Spectra of Single-Walled Carbon Nanotubes, *Science.* **2002**, *298,* 2361-2366.

2. R. Saito, G. Dresselhaus and M. S. Dresselhaus, Trigonal warping effect of carbon nanotubes, *Phys. Rev. B.* **2000**, *61,* 2981-2990.

3. S. Reich, C. Thomsen and P. Ordejon, Electronic band structure of isolated and bundled carbon nanotubes, *Phys. Rev. B.* **2002**, *65,* 155411.

4. A. Thess, R. Lee, P. Nikolaev, H. Dai, P. Petit, J. Robert, C. Xu, Y. H. Lee, S. G. Kim and et al., Crystalline ropes of metallic carbon nanotubes, *Science.* **1996**, *273,* 483-487.

5. T. W. Ebbesen and P. M. Ajayan, Large-Scale Synthesis of Carbon Nanotubes, *Nature.* **1992**, *358,* 220-222.

6. M. Endo, K. Takeuchi, S. Igarashi, K. Kobori, M. Shiraishi and H. W. Kroto, The Production and Structure of Pyrolytic Carbon Nanotubes (Pcnts), *J. Phys. Chem. Solids.* **1993**, *54,* 1841-1848.

7. J. Kong, H. T. Soh, A. M. Cassell, C. F. Quate and H. J. Dai, Synthesis of individual single-walled carbon nanotubes on patterned silicon wafers, *Nature.* **1998**, *395,* 878-881.

8. S. Maruyama, Y. Miyauchi, T. Edamura, Y. Igarashi, S. Chiashi and Y. Murakami, Synthesis of single-walled carbon nanotubes with narrow diameter-distribution from fullerene, *Chem. Phys. Lett.* **2003**, *375,* 553-559.

9. P. Nikolaev, M. J. Bronikowski, R. K. Bradley, F. Rohmund, D. T. Colbert, K. A. Smith and R. E. Smalley, Gas-phase catalytic growth of single-walled carbon nanotubes from carbon monoxide, *Chem. Phys. Lett.* **1999**, *313,* 91-97.

10. B. Kitiyanan, W. E. Alvarez, J. H. Harwell and D. E. Resasco, Controlled production of single-wall carbon nanotubes by catalytic decomposition of CO on bimetallic Co-Mo catalysts, *Chem. Phys. Lett.* **2000**, *317,* 497-503.

11. J. Lefebvre, S. Maruyama and P. Finnie, *Photoluminescence: Science and Applications,* 2008, pp. 287-318, In Book: A. Jorio, G. Dresselhaus and M. S. Dresselhaus (Editors), Carbon Nanotubes: Advanced Topics in the Synthesis, Structure, Properties and Applications.

50

12.   H. Kataura, Y. Kumazawa, Y. Maniwa, I. Umezu, S. Suzuki, Y. Ohtsuka and Y. Achiba, Optical properties of single-wall carbon nanotubes, *Synth. Met.* **1999**, *103*, 2555-2558.

13.   L. Yang and J. Han, Electronic Structure of Deformed Carbon Nanotubes. *Phys. Rev. Lett.* **2000**, *85*, 154-157.

14.   T. W. Odom, J. -L Huang, P. Kim and C. M. Lieber, Structure and Electronic Properties of Carbon Nanotubes, *J. Phys. Chem. B.* **2000**, *104*, 2794-2809.

15.   R. B. Weisman and S. M. Bachilo, Dependence of Optical Transition Energies on Structure for Single-Walled Carbon Nanotubes in Aqueous Suspension: An Empirical Kataura Plot. *Nano Lett.* **2003**, *3*, 1235-1238.

16.   T. Ando, Excitons in carbon nanotubes, *J. Phys. Soc. Jpn.* **1997**, *66*, 1066-1073.

17.   C. L. Kane and E. J. Mele, Ratio problem in single carbon nanotube fluorescence spectroscopy, *Phys. Rev. Lett.* **2003**, *90*, 207401.

18.   F. Wang, G. Dukovic, L. E. Brus and T. F. Heinz, The optical resonances in carbon nanotubes arise from excitons, *Science.* **2005**, *308*, 838-841.

19.   J. Maultzsch, R. Pomraenke, S. Reich, E. Chang, D. Prezzi, A. Ruini, E. Molinari, M. S. Strano, C. Thomsen and C. Lienau, Exciton binding energies in carbon nanotubes from two-photon photoluminescence, *Phys. Rev. B.* **2005**, *72*, 241402.

20.   Y. -Z Ma, L. Valkunas, S. M. Bachilo and G. R. Fleming, Exciton Binding Energy in Semiconducting Single-Walled Carbon Nanotubes, *J. Phys. Chem. B.* **2005**, *109*, 15671-15674.

21.   L. Lüer, S. Hoseinkhani, D. Polli, J. Crochet, T. Hertel and G. Lanzani, Size and mobility of excitons in (6,5) carbon nanotubes, *Nat. Phys.* **2009**, *5*, 54-58.

22.   S. Tretiak, S. Kilina, A. Piryatinski, A. Saxena, R. L. Martin and A. R. Bishop, Excitons and peierls distortion in conjugated carbon nanotubes, *Nano Lett.* **2007**, *7*, 86-92.

23.   L. Cognet, D. A. Tsyboulski, J. -D R. Rocha, C. D. Doyle, J. M. Tour and R. B. Weisman, Stepwise quenching of exciton fluorescence in carbon nanotubes by single-molecule reactions, *Science.* **2007**, *316*, 1465-1468.

24.   S. Berciaud, L. Cognet and B. Lounis, Luminescence decay and the absorption cross section of individual single-walled carbon nanotubes, *Phys. Rev. Lett.* **2008**, *101*, 077402.

25.   Y. -F Xiao, T. Q. Nhan, M. W. B. Wilson and J. M. Fraser, Saturation of the Photoluminescence at Few-Exciton Levels in a Single-Walled Carbon Nanotube under Ultrafast Excitation, *Phys. Rev. Lett.* **2010**, *104*, 017401.

26.   Y. Oyama, R. Saito, K. Sato, J. Jiang, Ge G. Samsonidze, A. Grueneis, Y. Miyauchi, S. Maruyama, A. Jorio, G. Dresselhaus and M. S. Dresselhaus, Photoluminescence intensity of single-wall carbon nanotubes, *Carbon.* **2006**, *44*, 873-879.

27.   C. D. Spataru, S. Ismail-Beigi, R. B. Capaz and S. G. Louie, Theory and ab initio calculation of radiative lifetime of excitons in semiconducting carbon nanotubes, *Phys. Rev. Lett.* **2005**, *95*, 247402.

28.   V. Perebeinos, J. Tersoff and P. Avouris, Effect of exciton-phonon coupling in the calculated optical absorption of carbon nanotubes, *Phys. Rev. Lett.* **2005**, *94*, 027402.

29.   H. Zhao, S. Mazumdar, C. X. Sheng, M. Tong and Z. V. Vardeny, Photophysics of excitons in quasi-one-dimensional organic semiconductors: Single-walled carbon nanotubes and pi-conjugated polymers, *Phys. Rev. B.* **2006**, *73*, 075403.

30.   I. B. Mortimer, L. -J Li, R. A. Taylor, G. L. J. A. Rikken, O. Portugall and R. J. Nicholas, Magneto-optical studies of single-wall carbon nanotubes, *Phys. Rev. B.* **2007**, *76*, 085404.

31.   J. Lefebvre, P. Finnie and Y. Homma, Temperature-dependent photoluminescence from single-walled carbon nanotubes, *Phys. Rev. B.* **2004**, *70*, 045419.

32.   J. Shaver, J. Kono, O. Portugall, V. Krstic, G. L. J. A. Rikken, Y. Miyauchi, S. Maruyama and V. Perebeinos, Magneto-optical spectroscopy of excitons in carbon nanotubes, *Phys. Status Solidi B.* **2006**, *243*, 3192-3196.

33.   J. Shaver, J. Kono, O. Portugall, V. Krstic, G. L. J. A. Rikken, Y. Miyauchi, S. Maruyama and V. Perebeinos, Magnetic brightening of carbon nanotube photoluminescence through symmetry breaking, *Nano Lett.* **2007**, *7*, 1851-1855.

34.   D. A. Tsyboulski, J. -D R. Rocha, S. M. Bachilo, L. Cognet and R. B. Weisman, Structure-dependent fluorescence efficiencies of individual single-walled cardon nanotubes, *Nano Lett.* **2007**, *7*, 3080-3085.

35.   J. Lefebvre, D. G. Austing, J. Bond and P. Finnie, Photoluminescence imaging of suspended single-walled carbon nanotubes, *Nano Lett.* **2006**, *6,* 1603-1608.

36.   S. -Y Ju, W. P. Kopcha and F. Papadimitrakopoulos, Brightly Fluorescent Single-Walled Carbon Nanotubes via an Oxygen-Excluding Surfactant Organization. *Science.* **2009**, *323,* 1319-1323.

37.   A. Hagen, G. Moos, V. Talalaev and T. Hertel, Electronic structure and dynamics of optically excited single-wall carbon nanotubes, *Appl. Phys. A.* **2004**, *78,* 1137-1145.

38.   F. Wang, G. Dukovic, L. E. Brus and T. F. Heinz, Time-resolved fluorescence of carbon nanotubes and its implication for radiative lifetimes, *Phys. Rev. Lett.* **2004**, *92,* 177401.

39.   M. Jones, W. K. Metzger, T. J. McDonald, C. Engtrakul, R. J. Ellingson, G. Rumbles and M. J. Heben, Extrinsic and intrinsic effects on the excited-state kinetics of single-walled carbon nanotubes, *Nano Lett.* **2007**, *7,* 300-306.

40.   S. Reich, M. Dworzak, A. Hoffmann, C. Thomsen and M. S. Strano, Excited-state carrier lifetime in single-walled carbon nanotubes, *Phys. Rev. B.* **2005**, *71,* 033402.

41.   G. N. Ostojic, S. Zaric, J. Kono, M. S. Strano, V. C. Moore, R. H. Hauge and R. E. Smalley, Interband recombination dynamics in resonantly excited single-walled carbon nanotubes, *Phys. Rev. Lett.* **2004**, *92,* 117402.

42.   F. Wang, G. Dukovic, E. Knoesel, L. E. Brus and T. F. Heinz, Observation of rapid Auger recombination in optically excited semiconducting carbon nanotubes, *Phys. Rev. B.* **2004**, *70,* 241403.

43.   V. C. Moore, M. S. Strano, E. H. Haroz, R. H. Hauge, R. E. Smalley, J. Schmidt and Y. Talmon, Individually suspended single-walled carbon nanotubes in various surfactants, *Nano Lett.* **2003**, *3,* 1379-1382.

44.   S. Berciaud, L. Cognet, P. Poulin, R. B. Weisman and B. Lounis, Absorption spectroscopy of individual single-walled carbon nanotubes, *Nano Lett.* **2007**, *7,* 1203-1207.

45.   J. G. Duque, M. Pasquali, L. Cognet and B. Lounis, Environmental and Synthesis-Dependent Luminescence Properties of Individual Single-Walled Carbon Nanotubes, *ACS Nano.* **2009**, *3,* 2153-2156.

46. T. Gokus, L. Cognet, J. G. Duque, M. Pasquali, A. Hartschuh and B. Lounis, Mono- and Biexponential Luminescence Decays of Individual Single-Walled Carbon Nanotubes. *J. Phys. Chem. C.* **2010**, *114*, 14025-14028.

47. L. Henrard, A. Loiseau, C. Journet and P. Bernier, Study of the symmetry of single-wall nanotubes by electron diffraction, *Eur. Phys. J. B.* **2000**, *13*, 661-669.

48. L. Henrard, A. Loiseau, C. Journet and P. Bernier, What is the chirality of singlewall nanotubes produced by arc discharge? An electron diffraction study, *Synth. Met.* **1999**, *103*, 2533-2536.

49. M. J. O'Connell, S. M. Bachilo, C. B. Huffman, V. C. Moore, M. S. Strano, E. H. Haroz, K. L. Rialon, P. J. Boul, W. H. Noon, C. Kittrell, J. Ma, R. H. Hauge, R. B. Weisman and R. E. Smalley, Band gap fluorescence from individual single-walled carbon nanotubes, *Science.* **2002**, *297*, 593-596.

50. G. Dukovic, B. E. White, Z. Y. Zhou, F. Wang, S. Jockusch, M. L. Steigerwald, T. F. Heinz, R. A. Friesner, N. J. Turro and L. E. Brus, Reversible surface oxidation and efficient luminescence quenching in semiconductor single-wall carbon nanotubes, *J. Am. Chem. Soc.* **2004**, *126*, 15269-15276.

51. A. Jorio, E. Kauppinen and A. Hassanien, *Carbon-Nanotube Metrology*, 2008, pp. 63-99, In Book: A. Jorio, G. Dresselhaus and M. S. Dresselhaus (Editors), Carbon Nanotubes: Advanced Topics in the Synthesis, Structure, Properties and Applications.

52. J. Shaver and J. Kono, Temperature-dependent magneto-photoluminescence spectroscopy of carbon nanotubes: evidence for dark excitons, *Laser Photon. Rev.* **2007**, *1*, 260-274.

53. R. J. Nicholas, I. B. Mortimer, L. J. Li, A. Nish, O. Portugall and G. L. J. A. Rikken, Temperature and magnetic field dependent photoluminescence from carbon nanotubes, *Int. J. Mod. Phys. B.* **2007**, *21*, 1180-1188.

54. R. B. Capaz, C. D. Spataru, P. Tangney, M. L. Cohen and S. G. Louie, Temperature dependence of the band gap of semiconducting carbon nanotubes, *Phys. Rev. Lett.* **2005**, *94*, 036801.

55. S. B. Cronin, Y. Yin, A. Walsh, Rodrigo B. Capaz, A. Stolyarov, P. Tangney, Marvin L. Cohen, Steven G. Louie, A. K. Swan, M. S. Unlu, B. B. Goldberg and M. Tinkham, Temperature dependence of the optical transition energies of carbon nanotubes: the role of electron-phonon coupling and thermal expansion, *Phys. Rev. Lett.* **2006**, *96*, 127403.

56.   D. Karaiskaj, C. Engtrakul, T. McDonald, M. J. Heben and A. Mascarenhas, Intrinsic and extrinsic effects in the temperature-dependent photoluminescence of semiconducting carbon nanotubes, *Phys. Rev. Lett.* **2006**, *96,* 106805.

57.   C. Fantini, A. Jorio, M. Souza, M. S. Strano, M. S. Dresselhaus and M. A. Pimenta, Optical transition energies for carbon nanotubes from resonant Raman spectroscopy: environment and temperature effects, *Phys. Rev. Lett.* **2004**, *93,* 147406.

58.   D. E. Milkie, C. Staii, S. Paulson, E. Hindman, A. T. Johnson and J. M. Kikkawa, Controlled switching of optical emission energies in semiconducting single-walled carbon nanotubes, *Nano Lett.* **2005**, *5,* 1135-1138.

59.   P. Finnie, Y. Homma and J. Lefebvre, Band-Gap Shift Transition in the Photoluminescence of Single-Walled Carbon Nanotubes, *Phys. Rev. Lett.* **2005**, *94,* 247401.

60.   D. A. Tsyboulski, S. M. Bachilo and R. B. Weisman, Versatile visualization of individual single-walled carbon nanotubes with near-infrared fluorescence microscopy, *Nano Lett.* **2005**, *5,* 975-979.

61.   Z. Wang, H. Pedrosa, T. Krauss and L. Rothberg, Determination of the Exciton Binding Energy in Single-Walled Carbon Nanotubes. *Phys. Rev. Lett.* **2006**, *96,* 047403.

62.   D. Tomanek, A. Jorio, M. S. Dresselhaus and G. Dresselhaus, *Introduction to the Important and Exciting Aspects of Carbon-Nanotube Science and Technology,* 2008, pp. 1-12, In Book: A. Jorio, G. Dresselhaus and M. S. Dresselhaus (Editors), Carbon Nanotubes: Advanced Topics in the Synthesis, Structure, Properties and Applications.

63.   E. S. Jeng, A. E. Moll, A. C. Roy, J. B. Gastala and M. S. Strano, Detection of DNA hybridization using the near-infrared band-gap fluorescence of single-walled carbon nanotubes, *Nano Lett.* **2006**, *6,* 371-375.

64.   P. W. Barone, R. S. Parker and M. S. Strano, In vivo fluorescence detection of glucose using a single-walled carbon nanotube optical sensor: Design, fluorophore properties, advantages, and disadvantages, *Anal. Chem.* **2005**, *77,* 7556-7562.

65.   H. Jin, D. A. Heller, M. Kalbacova, J-H Kim, J. Zhang, A. A. Boghossian, N. Maheshri and M. S. Strano, Detection of single-molecule H2O2 signalling from epidermal growth factor receptor using fluorescent single-walled carbon nanotubes, *Nature Nanotechnol.* **2010**, *5,* 302-309.

66. J-H Kim, D. A. Heller, H. Jin, P. W. Barone, C. Song, J. Zhang, L. J. Trudel, G. N. Wogan, S. R. Tannenbaum and M. S. Strano, The rational design of nitric oxide selectivity in single-walled carbon nanotube near-infrared fluorescence sensors for biological detection, *Nat. Chem.* **2009**, *1*, 473-481.

67. M. S. Arnold, S. I. Stupp and M. C. Hersam, Enrichment of single-walled carbon nanotubes by diameter in density gradients, *Nano Lett.* **2005**, *5*, 713-718.

68. M. S. Arnold, A. A. Green, J. F. Hulvat, S. I. Stupp and M. C. Hersam, Sorting carbon nanotubes by electronic structure using density differentiation, *Nat. Nanotechnol.* **2006**, *1*, 60-65.

69. E. H. Haroz, W. D. Rice, B. Y. Lu, S. Ghosh, R. H. Hauge, R. B. Weisman, S. K. Doorn and J. Kono, Enrichment of Armchair Carbon Nanotubes via Density Gradient Ultracentrifugation: Raman Spectroscopy Evidence. *ACS Nano.* **2010**, *4*, 1955-1962.

70. S. Ghosh, Sergei M. Bachilo and R. B. Weisman, Advanced sorting of single-walled carbon nanotubes by nonlinear density-gradient ultracentrifugation, *Nat. Nanotechnol.* **2010**, *5*, 443-450.

71. X. Tu, S. Manohar, A. Jagota and M. Zheng, DNA sequence motifs for structure-specific recognition and separation of carbon nanotubes, *Nature.* **2009**, *460*, 250-253.

72. X. Tu and M. Zheng, A DNA-based approach to the carbon nanotube sorting problem, *Nano Res.* **2008**, *1*, 185-194.

73. M. S. Strano, C. A. Dyke, M. L. Usrey, P. W. Barone, M. J. Allen, H. Shan, C. Kittrell, R. H. Hauge, J. M. Tour and R. E. Smalley, Electronic structure control of single-walled carbon nanotube functionalization. *Science.* **2003**, *301*, 1519-1522.

74. F. Huang, K. T. Yue, P. Tan, S-L Zhang, Z. Shi, X. Zhou and Z. Gu, Temperature dependence of the Raman spectra of carbon nanotubes. *J. Appl. Phys.* **1998**, *84*, 4022-4024.

75. V. A. Karachevtsev, A. Yu Glamazda, U. Dettlaff-Weglikowska, V. S. Kurnosov, E. D. Obraztsova, A. V. Peschanskii, V. V. Eremenko and S. Roth, Raman spectroscopy of HiPCO single-walled carbon nanotubes at 300 and 5 K. *Carbon.* **2003**, *41*, 1567-1574.

76. T. Uchida, M. Tachibana, S. Kurita and K. Kojima, Temperature dependence of the Breit-Wigner-Fano Raman line in single-wall carbon nanotube bundles. *Chem. Phys. Lett.* **2004**, *400*, 341-346.

77. A. Jorio, C. Fantini, M. S. S. Dantas, M. A. Pimenta, A. G. Souza Filho, Ge G. Samsonidze, V. W. Brar, G. Dresselhaus, M. S. Dresselhaus, A. K. Swan, M. S. Unlu, B. B. Goldberg and R. Saito, Linewidth of the Raman features of individual single-wall carbon nanotubes. *Phys. Rev. B.* **2002**, *66,* 115411.

78. M. Ichida, I. Umezu, H. Kataura, M. Kimura, S. Suzuki, Y. Achiba and H. Ando, Temperature dependence of time-resolved luminescence spectra for 1D excitons in single-walled carbon nanotubes in micelles, *J. Lumin.* **2005**, *112,* 287-290.

79. K. Koga, G. T. Gao, H. Tanaka and X. C. Zeng, Formation of ordered ice nanotubes inside carbon nanotubes, *Nature.* **2001**, *412,* 802-805.

80. Y. Maniwa, H. Kataura, M. Abe, S. Suzuki, Y. Achiba, H. Kira and K. Matsuda, Phase transition in confined water inside carbon nanotubes, *J. Phys. Soc. Jpn.* **2002**, *71,* 2863-2866.

81. Y. Maniwa, H. Kataura, M. Abe, A. Udaka, S. Suzuki, Y. Achiba, H. Kira, K. Matsuda, H. Kadowaki and Y. Okabe, Ordered water inside carbon nanotubes: formation of pentagonal to octagonal ice-nanotubes, *Chem. Phys. Lett.* **2005**, *401,* 534-538.

82. S. Moritsubo, T. Murai, T. Shimada, Y. Murakami, S. Chiashi, S. Maruyama and Y. K. Kato, Exciton Diffusion in Air-Suspended Single-Walled Carbon Nanotubes, *Phys. Rev. Lett.* **2010**, *104,* 247402.

83. D. A. Tsyboulski, E. L. Bakota, L. S. Witus, J. -D R. Rocha, J. D. Hartgerink and R. B. Weisman, Self-Assembling Peptide Coatings Designed for Highly Luminescent Suspension of Single-Walled Carbon Nanotubes, *J. Am. Chem. Soc.* **2008**, *130,* 17134-17140.

84. Y-Z Ma, L. Valkunas, S. L. Dexheimer, S. M. Bachilo and G. R. Fleming, Femtosecond spectroscopy of optical excitations in single-walled carbon nanotubes: evidence for exciton-exciton annihilation, *Phys. Rev. Lett.* **2005**, *94,* 157402.